Journal of Applied Polymer Science

REVIEW

An Overview of Luminescent Bio-Based Composites

Ricardo J. B. Pinto,[1] Luís D. Carlos,[2] Paula A. A. P. Marques,[3] Armando J. D. Silvestre,[1] Carmen S. R. Freire[1]

[1]Department of Chemistry, CICECO, University of Aveiro, 3810-193 Aveiro, Portugal
[2]Department of Physics, CICECO, University of Aveiro, 3810-193 Aveiro, Portugal
[3]Department of Mechanical Engineering, TEMA, University of Aveiro, 3810-193 Aveiro, Portugal
Correspondence to: C. S. R. Freire (E-mail: cfreire@ua.pt)

ABSTRACT: The development of inorganic/organic composite materials represents a fast-growing interdisciplinary area in materials science and engineering. In this topic, a key idea is the production of composites comprising biopolymers and functional inorganic phases that could replace conventional materials in several high-technology applications. Following this concept, the use of different polymers from renewable sources, such as cellulose, starch, alginate, and chitosan, have gained great relevance because of their renewable nature, potential biocompatibility, and biodegradability, as well as specific physicochemical properties. The combination of these biopolymers with different fillers (including inorganic nanoparticles (NPs), clusters, or ions) allows the design of innovative bio-based materials with specific and/or improved properties, namely, optical, mechanical, and barrier properties, luminescence, and biological properties (as antimicrobial activity and biocompatibility). This review will focus on the most important synthetic approaches, properties, and applications of luminescent bio-based composites obtained by combining different biopolymers and fillers. © 2014 Wiley Periodicals, Inc. J. Appl. Polym. Sci. **2014**, *131*, 41169.

KEYWORDS: composites; nanoparticles; nanocrystals; optical properties

Received 8 May 2014; accepted 17 June 2014
DOI: 10.1002/app.41169

INTRODUCTION

History shows that breakthroughs in the performance or cost of functional materials can drive cycles of disruptive growth. A new revolution in materials has been taking shape around the world during the past few decades. Scientists are perfecting new ways to manipulate matter aiming to produce advanced materials with unheard-of attributes that could enable innovations in fields ranging from infrastructure construction to medicine, passing through packaging materials. The concepts involved in polymers and composites as advanced materials hardly come as recent revelations. Nature itself has made good use of structural natural polymers, as cellulose, and produced strong polymeric fibers, as silk in spider webs, long before synthetic chemists arrived on the scene.

Currently, composite materials have a strong positive impact on our present and future economy, the state of environment, the quality of our health, the efficiency of infrastructures, and the security of our society. The term composite refers to materials made from two or more constituent materials with significantly different physical or chemical properties, that when combined, produce a material with characteristics different from the individual components. The benefits derived from creating a composite material can include higher flexibility and mechanical strength, a larger temperature range of usability, increased durability, improved electrical, magnetic or redox properties, or creating complex multifunctional domains within the same material. Nowadays, composite materials should meet certain environmental requirements, such as being recyclable and safe. Hence, the use of abundant, low-cost, and environmentally friendly biopolymers, such as polysaccharides, to synthesize composite materials is gaining much attention. Our research group has a long history on the design/development of polymers from renewable resources[1–3] and of new sustainable composite materials.[4–7] In addition, several functional composite materials have been prepared by the association of biopolymers with inorganic materials such as noble metals[8–10] and metal oxides.[11–13]

Interest in luminescent bio-based composites has grown considerably during the last decade, with the concomitant fabrication of materials with tunable attributes offering modulated properties. The potential of these materials relies on exploiting the synergy between the intrinsic characteristics of bio-based polymers (including cellulose, chitosan, gelatin, starch, alginate, carrageenan, and dextrin as well as some derivatives) and the luminescence features of the optically active centers (essentially

Ricardo J. B. Pinto was born in 1981 (Alijó, Portugal), he graduated in Chemistry at University of Porto (2004) and finished is Master degree in Materials in 2008 at the University of Aveiro (UA, Portugal). In 2012, he obtained his PhD at the same university. Currently, he is a postdoctoral researcher at the Associate Laboratory's CICECO and TEMA (UA, Portugal) and their research interests are focused on the development of new functional bio-based hybrid composites.

Luís D. Carlos (1964) got his Ph.D. in physics from the University of Évora in 1995. Currently, he is Full Professor at the Department of Physics (University of Aveiro), member of the Lisbon Academy of Sciences (Physics section, 2011) and vice-director of CICECO at Aveiro (2009). His current scientific interests include light emission of organic-inorganic hybrids, silicates, MOFs and nanocrystals; applications of hybrids in green photonics; nanothermometry, among many others.

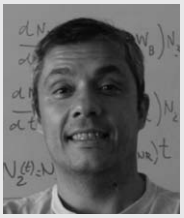

Paula A. A. P. Marques is Principal Researcher at the University of Aveiro, Portugal, being the Scientific Coordinator of the Nanotechnology Research Division of the Mechanical Engineering Department. She is graduated in Chemistry, master in Physics and Chemistry Teaching and doctorate in Materials Science Engineering. Paula's main field of research is dedicated to the engineering and development of new nanostructured materials (e.g. graphene based nanocomposites with applications in the biomaterials and biosensors area).

Armando J. D. Silvestre born in 1968 (Aveiro, Portugal), graduated in Chemistry in 1990, got his PhD in 1994 and the Habilitation degree in 2008 at the University of Aveiro (UA, Portugal). He is currently Associate Professor at the Chemistry Department of UA. His research interests comprise the extraction, characterization and valorisation of biomass components in areas such as low molecular weight bioactive components, bio-based polyesters, and (nano)cellulose fibres-based nanocomposite materials.

Carmen S. R. Freire born in 1976 (Caracas, Venezuela), graduated in Industrial Chemistry in 1998 and obtained her PhD in Chemistry in 2003 at the University of Aveiro (UA, Portugal). She is currently Principal Researcher at the Associate Laboratory CICECO (University of Aveiro-UA). Her research interests are centered on the chemistry of polymers from renewable resources (characterization and application), development of new sustainable composite materials, nanostructured biomaterials and generally on the chemistry of natural compounds.

organic dyes, quantum dots [QDs] and trivalent lanthanide ions [Ln^{3+}]). Promising applications may be envisaged, such as biomedical and chemical actuators and sensors, optical devices, security materials, bioimaging agents, and high technological materials (information encryption, flat displays, and energy conversion), opening up exciting directions in materials science and related technologies.[14–17]

Luminescence is a general term which describes any nonthermal processes in which energy is emitted at a different wavelength from that at which it is absorbed. Photoluminescence results from excitation by photons, and the interaction mechanisms between the photon and the matter depend on the photon energy, among other aspects. When the photon energy of the incident radiation is lower than the energy difference between two electronic states, the photons are not really absorbed, and the material is transparent to such radiation energy. For higher photons energy, absorption occurs and the low energy electrons will make a transition between two electronic energy levels. The excess of energy will be dissipated through vibrational processes

that occur throughout the near infrared (NIR) spectral region. Then, the excited atoms may return to the original level through radiative (e.g., with the spontaneous emission of a photon) and nonradiative transitions.

The basic luminescence principles depend on the nature of the optically active center and are distinct from organic dyes to QDs, transition metals, or Ln^{3+} ions. In organic dyes, after optical absorption, the electrons will be excited to a singlet or a triplet state, and the luminescence is generated by a transition from those levels to the ground singlet. It should be noted that transitions involving a triplet state are forbidden by the spin selection rule (allowed transitions must involve the promotion of electrons without a change in their spin, $\Delta S = 0$) that can be relaxed through strong spin–orbit coupling.

In semiconducting QDs, the ground state is commonly referred to electrons in the valence band (completely filled with electrons). The excited state is usually localized in the conduction band that is separated from the valence band by an energy gap named the band gap. In direct semiconducting QDs, the energy released by a de-excitation from the lowest energy state of the conduction band (LUMO) and the highest energy state of the valence band (HOMO) is nearly equal to the band gap. QDs are nanoparticles with dimensions in the range of 1–30 nm with electronic properties that are intermediate between those of bulk semiconductors and of discrete molecules. The fascinating changes of their optical and electronic properties (e.g., in optical absorption, exciton energies, and electron–hole pair recombinations) are determined by factors such as size (surface-to-volume ratio and quantum confinement effects), shape, defects, impurities, and crystallinity.

In transition metal and Ln^{3+} ions, the light emission is governed by transitions between levels of a given configuration, *d–d* and *f–f* transitions, respectively. Laporte's parity selection rule implies that electric–dipole (ED) transitions between states of the same shell (same parity) are forbidden. This parity rule is relaxed when the ions are under the influence of a ligand field (the static electric field produced by the ions surrounding charge distribution). Noncentrosymmetric interactions promote the mixing of opposite-parity wave functions into the *d* and *f* wavefunctions (or the coupling of the electronic transitions with vibrations of suitable symmetry), and the ED transitions become partially allowed, the so-called induced (or forced) ED transitions. Magnetic dipole transitions are allowed; however, their intensity is generally weak.

The ground-state electronic configuration of transition metal and Ln^{3+} ions are d^N $(0 \leq N \leq 10)$ and f^N $(0 \leq N \leq 14)$, where N is the number of electrons. For Ln^{3+} ions, the *f* orbital lie inside the ion (inner orbital) and is shielded from the surrounding neighborhoods by the filled $5s^2$ and $5p^6$ subshells of the Xe core. The influence of the ligand field (and of the host lattice) on the *f–f* transitions is therefore much smaller than in the *d–d* transitions of transition metals. In fact, the ligand field in Ln^{3+} ions (10^2 cm^{-1}) is typically two orders of magnitude smaller than in transition metals (10^4 cm^{-1}); however, it is the key to explain the chemical and spectroscopic properties of these ions. The ligand filed destroys the spherical symmetry of the free ion electronic structure, and the energy levels are marked $^{2S+1}L_J$ (Russell-Saunders coupling), where S is the total spin quantum number, L is the total orbital angular momentum, and J is the total angular momentum, $L + S \geq J \geq |L - S|$. Energy levels corresponding to definitive values of L and S are called spectral terms. Capital letters of the Latin alphabet are usually used for denoting those terms as 0 (S), 1 (P), 2 (D), 3 (F), 4 (G), and so forth. The degeneracy of these terms is represented by $2S + 1$ $(L \geq S)$ or $2L + 1$ $(L < S)$ and are partly lifted by the ligand field depending on the exact point symmetry group of the metal ion site. For transition metals, ligand field levels are denoted as ^{2S+1}X, where X may be A (no degeneracy), E (twofold degeneracy), and T (threefold degeneracy). Subscripts are related to the local symmetry of the charge distribution around the ion. For Ln^{3+} ions, the ligand field split the $^{2S+1}L_J$ levels into a maximum of $2J + 1$ Stark components, depending on the local symmetry of the ion. Because of the weak ion–ligand interaction, the intraconfigurational *4f* transitions are very sharp (bandwidths of 10–20 nm, quasi-atomic spectra), in contrast to the much broad emission typical of transition metals. For more details, the reader is referred to Refs. 18–21.

In light of the huge development in this field, it is imperative to summarize the most relevant research results concerning luminescent bio-based composites. This review outlines the distinct biopolymers used and their correspondent luminescent fillers, focusing the respective preparative methods and potential applications (Table I). Furthermore, the major concerns concerning the environmental impact of some luminescent fillers as the new advances and opportunities on this area will be put in perspective on this work.

CELLULOSE-DERIVED LUMINESCENT MATERIALS

Cellulose is the most abundant natural polymer, because it is the main component of plant cell walls, and therefore constitutes a very important and abundant renewable resource for the development of innovative materials.

Conventional Plant Cellulose-Based Materials

Plant cellulose, in the form of microcrystalline cellulose,[22–25] Kraft pulp fibers,[26] paper fibers,[27–29] regenerated fibers,[30,31] hydrogels,[32–36] transparent sheets,[37] nanocrystals,[38,39] and nanofibrillated cellulose (NFC),[40] has been extensively used as biopolymeric templates for the development of innovative luminescent materials because of its abundance and the chemical and structural functionalities it offers.

Most of the studies dealing with luminescent cellulose-based materials involved the combination of cellulose with different inorganic compounds; however, the first reports on this topic investigated the photochemistry of organic probes, namely, benzophenone,[22,23] fluorenone,[23] and 2,2′-cyanines[24] adsorbed onto microcrystalline cellulose. Luminescence studies revealed that whenever these dye molecules are entrapped into the cellulose chains and in close interaction with the substrate, a strong quenching effect occurs at room temperature. For instance, for fluorenone, the fluorescence quantum yields ($^1/_4$F) were about 0.10 when solvents which do not swell cellulose (e.g., dichloromethane, cyclohexane, and benzene) were used for sample

Table I. Summary of the Distinct Biopolymers, Luminescent Fillers, Methodologies, and Potential Applications of the Most Relevant Luminescent Bio-Based Composites Described in the Literature

Biopolymer	Type/morphology	Luminescent filler	Preparative methods	Potential Applications	Reference
Cellulose	Microcrystalline cellulose	Benzophenone, 2,2′-cyanines, fluorenone, iridium complexes	Solution absorption followed by solvent removal, mechanical mixing, and blending	Oxygen sensors	22–25
	Cellulose fibers (Kraft pulp fibers)	Doped ZnS nanocrystals	Solution absorption followed by solvent removal	Photovoltaic cells and light-emitting diodes	26
	Cellulose fibers (paper substrate)	CdSeS/ZnS QDs, nanofibrous silicon	Solution absorption followed by solvent removal, magnesiothermic reduction	Bioassays, photoelectronic sensors and devices	27–29
	Regenerated fibers	Eu^{3+} doped NPs	Dry–wet spinning	Security-patterned papers and textiles	30,31
	Hydrogels	QDs, Eu^{3+}, and Tb^{3+}	Dissolution of cellulose in an appropriated solvent followed by the addition of the luminescent filler	Bioassays and biomonitoring	32–36
	Transparent sheets	Eu^{3+}	Solvent casting	Optical filters and display technologies	37
Nanocellulose	Nanocrystals	Carbon nanotubes, silicon NPs	Self-assembly followed by LbL, blending	Multifunctional materials	38,39
	Nanofibrillated cellulose	Ag nanoclusters	Functionalization mediated by PMMA	Multifunctional materials	40
	Bacterial cellulose	Eu^{3+} complexes, CdSe, and CdSe/ZnS QDs	Solution absorption followed by solvent removal, *in situ* synthesis, and assembly via cellulose-binding proteins	Phosphors and UV–visible energy-converting devices, sensors, and security papers	41–43
Cellulose derivatives	Ethylcellulose	$CdCl_2$, platinum octaethylporphyrin, complex indicator systems, QDs, iridium(III) complex, Eu^{3+}, and Ce^{3+}	Solution absorption followed by solvent removal, casting, and knife coating	H_2S determination, oxygen sensors, pCO_2 and pO_2 sensors, biosensing, and fluorescent lamps	44–51
	Cellulose acetate	Ruthenium diimine complexes, chemiluminescent reagent, fluorescein isothiocyanate, CdSe/CdS nanorods	Casting, solution absorption followed by solvent removal	Oxygen sensors, biosensing (human AFP)	52–56
	Carboxymethylcellulose	Salicyl flourones, Ag NPs, ZnS NPs, and CdS QDs	Sol–gel, *in situ* synthesis using microwave irradiation, casting, and *in situ* capping	Hg and Ag sensors, advanced nanostructured materials, security papers, and iodate sensors	57–61
	Cellulose acetatebutyrate	Platinum octaethylporphyrin	Solvent casting	Oxygen sensors	45,46
	Nitrocellulose	Eu^{3+} and Ce^{3+}	Calcination	Fluorescent lamps	51
	Hydroxypropylcellulose	Eu-doped YVO_4	Spin coating followed by calcination	–	62

Table I. *Continued*

Biopolymer	Type/morphology	Luminescent filler	Preparative methods	Potential Applications	Reference
	Cyanoethylcellulose	CuInSe QDs	Casting	Solid-state lighting emission diodes, light-emitting devices, and laser displays	63
Chitosan	Coatings for electrodes	Metal complex ($Ru(bpy)_3^{2+}$)	Blending of components	Electrochemiluminescence optic sensor	64–66
		PtAg@carbon nanocrystals	Blending of components under sonication	Biosensor and clinical disease diagnostics	67
		QDs (CdTe, CdSe, and QDs-coated silica NPs)	Blending of components	Dopamine sensor, electrochemiluminescence optic sensor, and clinical and molecular diagnostics	68–71
	Self-standing films	Metal complex (Eu^{3+})	Blending of components	Sensors	72
		QDs (CdTe)	Blending of components	Biomedical field	73
		Metal clusters (Au)	Soaking of the chitosan film on Au clusters solution	Security, medical, environmental remediation, and Cu^{2+} sensor	74,75
	Microspheres and nanospheres	QDs (CdSe/ZnS and CdSe/CdS)	Blending of components, electrostatic assembly	Bioassays, cell imaging, and sensors	76–78
		Metal complex ($Ln_{0.33}^{3+}$ Gd_x^{3+}/$[Mo(CN)_8]^{3+}$)	Incorporation of previously prepared metal complex into pristine porous chitosan beads	Imaging probes	79
		Metal complex (LaF_3 : Eu^{3+})	Coprecipitation	Intracellular labeling or measurements	80
		Metal complex ($NaYF_4$: Yb/Er)	Blending of components	Detection and molecular diagnosis of lung cancer	81
		Metal complex (Eu^{3+} and Tb^{3+})	Sol–gel process and radical polymerization	Biological applications in diagnostics and therapy	82,83
		Metal clusters (Au and Ag)	LbL and nonsolvent-aided counter ion complexation	Bioimaging, security, and medical and environmental remediation	75,84
		QDs (CdTe)	Blending of components under sonication/electrostatic assembly and subsequent polymerization	Insulin delivery, cell imaging, antidiabetic investigation of dietary supplements, and bioactive molecule carriers	85–87
		QDs (InGaP/ZnS)	Blending of components with further QDs activation	Bioimaging	88
		QDs (Zn–Ag–In–Se)	Loading of QDs on RGD peptide modified chitosan-based micelles	Bioimaging	89
		QDs (ZnS and ZnS : Mn^{2+})	Blending of components	Biomedical field, biosensor	90,91
		Metal oxide (ZnO and ZnO/Eu^{3+})	Blending of components	Printed security	92

Table I. *Continued*

Biopolymer	Type/morphology	Luminescent filler	Preparative methods	Potential Applications	Reference
		Metal NPs (Ag, Ni_3Se_2, and Au nanorods)	*In situ* synthesis, γ-ray-assisted synthesis and covalent binding with functionalized Au nanorods	Biosensing, drug delivery, noninvasive imaging, and photothermal-based applications	93–95
		QDs (CdS)	Blending of components and layer-by-layer assembly	Sensors	96
Chitosan derivatives	Carboxymethyl chitosan	Metal complexes (Yb^{3+}/Tm^{3+}/Er^{3+})	Hydrothermal process	Biomedical field (cell imaging)	97
		QDs (CdTe/CdS and CdSe/ZnS)	Blending of components	Biomedical field (cell imaging)	98,99
	Water-soluble chitosan	QDs		Biosensors	100
		Lanthanopolyoxometalates	Blending of components	–	101
Gelatin	Films	Ag clusters	Femtosecond-laser-induced reduction of silver oxide NPs with subsequent casting	Spectroscopic probes	102
		Single-walled carbon nanotubes (SWCNTs)	Dispersion of individual SWCNTs on the matrix	Photoelectric and light emitting material	103
		QDs (CdSe, CdSe/ZnS, and CdSe/CdS)	Blending of components	–	104,105
		Rodhamine 6G/Ag NPs	Blending of components followed by drying	Biosensor	106
	Electrospun fibers	$NaYF_4$: Yb^{3+}, Er^{3+}@$mSiO_2$	Dispersion of inorganic fillers in poly(ε-caprolactone)–gelatin followed by electrospinning of the mixture	Dual drugs delivery system for wound healing or implant in surgery	107
	Microspheres and nanospheres	QDs (CdSe, CdTe, and CdS)	Desolvation method and blending of components	Biological imaging	108–112
		QDs (CdSe/HgSe and CdSe/Ag_2Se)	Colloidal synthesis	–	113
		Metal clusters (Au)	Blending of components	NIR optical imaging	114
		Metal complex (Eu^{3+} and Tb^{3+})	Hydrothermal process	–	115
		Carbon dots	Hydrothermal process	Bioscience, optical devices, information encryption, and energy conversion	116
Starch	Films	Organic dye (fluorescein)	Ring-opening reaction with 3-epoxypropoxy fluorescein	Polymeric temperature/pH indicators	117
	Powder	QDs (ZnSe and CdTe)	LbL assembly	Semiconductor QD-based light emission diodes	118
		Metal complex (YVO_4 : Sm and YVO_4 : Dy)	Complex-based sol–gel method	High-definition flat displays	119

Table I. *Continued*

Biopolymer	Type/morphology	Luminescent filler	Preparative methods	Potential Applications	Reference
	Flower-like nanostructure	Metal oxide (ZnO)	Sonochemical method	-	120
	Nanospheres	Metal oxide (ZnO)	Laser ablation of a ZnO plate in starch solution	Bioimaging agent, biosensors, and as drug delivery vehicles	121
	Nanospheres and elongated nanostructures	QDs (CdSe)	Nonorganometallic method	-	122
	As capping agent	QDs (CdSe and PbSe)	Blending of components	Solar cells	123
DNA	Membrane film	Metal complex (Eu^{3+})	Blending of components	Optic solid-state electrochemical devices	124
Alginate	Aerogel, hydrogel, and xerogel	Metal complex (Eu^{3+} and Tb^{3+})	Blending of components	Tunable light emitters	125
	Nanostructures	QDs (CdS and CdTe)	Ligand exchange	Optical devices	126
	Microparticles	QDs (CdTe)	LbL assembly	Biomedical applications	127
Carrageenan	Gels	Metal complex (Eu^{3+})	Blending of components	-	128
Dextrin	Microspheres	Metal complex (Eu^{3+})	Spray drying	-	129

preparation, whereas for those which efficiently swell cellulose (e.g., dioxane, acetone, ethanol, and methanol), the $^1/_4$F was around 0.01.[23] These values are approximately one order of magnitude higher than those attained in solution, demonstrating the importance of the rigid dry cellulose matrix in decreasing the nonradiative pathways of deactivation of the (ð,ð*)fluorenone first excited singlet state. In fact, spectroscopic studies (X-ray photoelectron spectroscopy (XPS) or Fourier transform infrared (FTIR) spectroscopy) evidenced strong hydrogen bonding between the probe dye molecules and the cellulose chains.

Recently, Habibagahi et al.[25] developed water-based oxygen sensor films by combination of colloidal microcrystalline cellulose and a luminescent cyclometalated iridium complex chemically bound to a water-soluble amine-functionalized polymer (quantum yield of emission and excited state lifetime; $\varphi_{em} = 0.23$ and $\tau = 20.6$ μs, respectively). Oxygen sensitivities of the obtained films were determined as a function of complex : microcrystalline cellulose ratio and complying with Stern-Volmer kinetics. The ideal oxygen-sensor film composition was found to be 1 : 1, which had an oxygen sensitivity of 0.502 over an atmospheric pressure range of 0.007–45 psi. Temperature sensitivity (percentage loss of intensity per degree Celsius) of this film was -1.1 and -1.4% $^\circ C^{-1}$ at vacuum and 1 bar atmospheric pressure, respectively.

In another ground-breaking study, Small and Johnston[26] developed photoluminescent cellulose fibers by coating bleached Kraft fibers with ZnS nanocrystals (about 15 nm in diameter) doped with 0.1–2 wt % of Mn^{2+} and Cu^{2+}. XPS analysis indicated that strong bonding between the cellulose fibers and the nanocrystals occurred. However, the inherent mechanical properties of the fibers and their ability to be shaped into a paper sheet were preserved but imparted with the photoluminescent properties of the coatings, that is, the emissions were at around 600 nm and 530 nm for Mn^{2+}- and Cu^{2+}-doped nanocrystals, respectively.

Recently, Kim et al.[27] reported an original methodology for the immobilization of brightly luminescent CdSeS/ZnS QDs on cellulose fibers of paper substrates for Forster resonance energy transfer (FRET)-based bioassays of proteolytic activity. Steady-state and time-resolved fluorescence characterization of FRET between immobilized QDs (donors) and self-assembled dye-labeled peptides (acceptors) within the paper matrix showed a substantial enhancement in energy transfer efficiency. Changes in the dye/QD photoluminescence ratio endorsed the tracking of proteolytic activity, comprising the effect of increasing amounts of aprotinin, a potent inhibitor of trypsin. Therefore, the combination of QDs, a cellulosic substrate, and enhanced FRET has enormous potential for the development of innovative bioassays. In a similar way, Niu et al.[28] described the preparation of luminescent cellulose sheets prepared by self-assembly of cadmium selenide (CdSe) NPs covered with trioctylphosphine oxide and 1-hexadecylamine onto ultrathin titania film precoated cellulose fibers of classic filter paper. The authors claimed that in this process, the cellulose nanofibers of the filter paper were previously coated with a titania layer; however, the

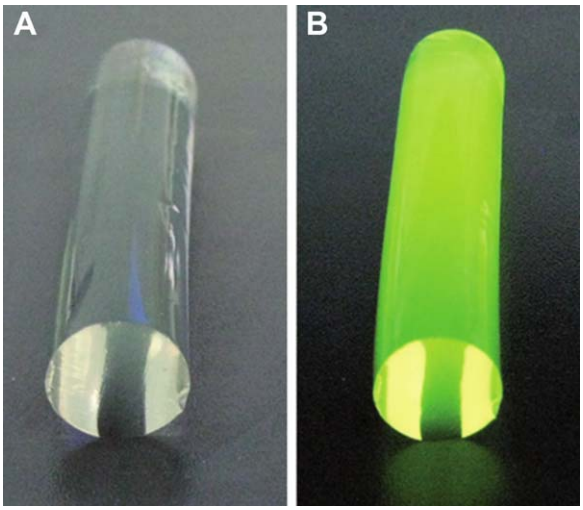

Figure 1. Photographs of cellulose QDs hydrogel with 0.06 wt % QDs (3.0 nm) under visible light (A) and a 302-nm UV lamp (B). (Adapted from Ref. 32, with permission from Royal Society of Chemistry.). [Color figure can be viewed in the online issue, which is available at wileyonlinelibrary.com.]

conditions used do not allow the fibrillation of the cellulose fibers and therefore their availability in the coating step. In fact, the scanning electron microscopy (SEM) and transmission electron microscopy results showed that the resulting luminescent films maintained the morphology of the initial cellulose substance, that is, the typical micrometric cellulose fibers.

In a completely distinct strain, photoluminescent hierarchical nanofibrous crystalline silicon was prepared by low-temperature magnesiothermic reduction of nanosilica replica of cellulose fibers (commercial filter paper and cotton).[29] This porous silicon material shows strong blue or red photoluminescence when irradiated with UV or green light, being suitable for numerous applications such as fabrication of optoelectronic sensors and devices. However, in this strategy, cellulose fibers are only used as templates not as constituents of the final material.

Luminescent-regenerated cellulose fibers were obtained by dry–wet spinning of 8 wt % cellulose solutions in *N*-methylmorpholine *N*-oxide modified with ZrO_2 (0.5 mol % of Eu^{3+}) stabilized by Y_2O_3 (7 mol%)[30] or Eu^{3+}-doped gadolinium oxyfluoride (5 mol % of dopant).[31] These fibers contained from 0.5 to 10% w/w of luminescent modifier, and the intensity of the optical signals was harshly dependent on its amount in the cellulose matrix. X-ray diffraction (XRD) measurements suggested that the presence of these additives did not affect the crystalline structure of cellulose but promoted a considerable decrease of the fibers tenacity (up to 40% for 5% of Eu^{3+}-doped NPs).[31] Cellulose fibers with such properties can be used for the security pattern of documents, papers, and textile products.

Strongly fluorescent hydrogels with CdSe/ZnS QDs embedded in cellulose matrices were successfully fabricated by Chang et al.[32] (Figure 1). FTIR spectroscopy, photoluminescence spectroscopy, and microscopy analysis revealed that the cellulose networks in the hydrogels played a significant role in the protection of the CdSe/ZnS NPs structure and maintenance of the QDs characteristics. These cellulose/QDs hydrogels exhibited strong photoluminescence emission, with different color depending on the size of the QDs, relatively high photoluminescent quantum yields (up to 34%), and good transparency and compressive strength (45–49 kPa), being promising for applications in the fields of biological labeling and fluoroimmunoassays.

In a different study, Zhou and Wang[33] described the fabrication of transparent cellulose hydrogel films with narrow emission via the simple assembly of terbium silica xerogels into cellulose hydrogels (prepared by dissolution of microcrystalline cellulose in an ionic liquid followed by application of the obtained viscous solution onto a glass surface and washing of the excess of the ionic liquid with water). When immersed in NO_2^- solutions, their luminescence quenching effects could be rapidly perceived and therefore can be used as portable tools to monitor nitrite in the biological and environmental fields. Following a similar approach, the same research group also reported the preparation of luminescent Cu^{2+} probes based on Eu^{3+} and Tb^{3+} emissive transparent cellulose hydrogels[34] and luminescent hydrogels based on Tb^{3+}–human serum albumin that showed reversible "on–off" switch signal changes based on pH variations.[35] As a final point regarding cellulose hydrogels, photoluminescent lanthanide (Eu^{3+}, Tb^{3+}, Sm^{3+}, and Dy^{3+}) phosphors were successfully obtained, at low temperature (70 °C), using simultaneous supersonic and microwave irradiation.[36] These lanthanide-based phosphors were subsequently incorporated in cellulose hydrogels that were similarly strongly emissive on excitation at 254 nm.

Van Opdenbosch et al.[37] prepared flexible, transparent, and luminescent cellulose sheets through the addition of $EuCl_3$ to a cellulose solution in DMAc/LiCl, followed by tape casting and treatment of the ensuing films with an aqueous solution of NH_4F. Scanning electron micrographs of the obtained sheets displayed EuF_3 particles with diameters in the range of 200–500 nm. Assessment of the emission characteristics of these sheets showed the typical band pattern between 580 and 700 nm of Eu^{3+} phosphors. This strategy opens new materials design routes to prepare transparent and functional materials for applications in optical filters and display technologies. However, the use of more environmentally friendly solvent systems, as ionic liquids or urea/aqueous solutions, should be considered aiming to establish truly green and efficient processes.

Nanocellulose-Based Materials

The use of nanosized cellulose substrates, such as cellulose nanocrystals and NFC, obtained from acid hydrolysis and mechanical treatment of plant fibers, respectively, opens the doorway to prepare functional nanomaterials with improved properties that could not be achieved by conventional plant fibers.

For example, Olivier et al.[38] prepared highly stable single-walled carbon nanotubes (SWCNTs) dispersions (about 24% of SWCNTs) by ultrasonication in cellulose nanocrystals aqueous colloidal suspensions. SWCNTs and cellulose nanocrystals self-assemble into hybrids characterized by the alignment of several cellulose crystals along the SWCNT axis probably due to short-

range hydrophobic interactions occurring between the SWCNTs and specific crystalline faces of the cellulose crystals. These SWCNT/cellulose nanocrystals dispersions were subsequently used to create homogeneous multilayered thin films, using a layer-by-layer (LbL) methodology with polyallylamine hydrochloride as the polyelectrolyte, which exhibits a NIR luminescence signal due to isolated and well-separated nanotubes. In a different study, luminescent nanocomposites based on silicon NPs and nanocrystalline cellulose were developed by the addition of porous silicon powder to the cellulose nanocrystals suspension followed by ultrasound dispersion of the ensuing mixture.[39] The nanocomposite samples were finally shaped under pressure (0.26 MPa) from the solid mixture obtained after evaporation of the solvent at room temperature. The assessment of the effect of temperature and gas phase oxidation with ozone on the luminescent properties of the nanocomposites suggested a high stability of the luminescent properties.

Quantum clusters of noble metals recently emerged as a new category of luminescent materials because of their low cytotoxicity, excellent photostability, and high quantum yield. The functionalization of NFC using fluorescent silver nanoclusters as a way to prepare novel functional nanocellulose/nanocluster composites was recently reported.[40] This functionalization was mediated by poly(methacrylic acid) that simultaneously protected the silver nanoclusters and allowed hydrogen bonding with cellulose, as tentatively suggested by the authors. The ensuing composites retained the attractive properties of silver nanoclusters, namely, fluorescence and antibacterial activity. However, only these properties were evaluated and a more detailed study (e.g., in terms of mechanical performance and thermal stability) will be required to evaluate the properties of the ensuing materials.

Nanocellulose substrates can also be produced by bacteria, the so-called bacterial cellulose (BC) or microbial cellulose, in the form of a tridimensional network of nanofibers. BC membranes have also been used as nanostructured substrates for the preparation of luminescent bio-based materials because of their singular morphology and mechanical properties.[41,42] Specifically, Caiut et al.[41] prepared luminescent BC composite membranes by the incorporation of ethanolic solutions of different europium compounds, namely, [Eu(4,4,4-trifluoro-1-phenyl-1,3-butanedione)$_3$(H_2O)$_2$], [Eu(4,4,4-trifluoro-1-phenyl-1,3-butanedione)$_3$(dibenzylsulfoxide)$_2$], [Eu(4,4,4-trifluoro-1-phenyl-1,3-butanedione)$_3$(*p*-tolyl sulfoxide)$_2$], and [Eu(4,4,4-trifluoro-1-phenyl-1,3-butanedione)$_3$(phenyl sulfoxide)$_2$], into the BC network followed by drying. The obtained membranes were semitransparent, self-sustainable, and showed strong emission under UV excitation. The antenna hole played by the ligands was perceived to be more efficient in the composite membranes than in the precursor complexes, which by themselves are also strong red emitter compounds. These novel functional BC membranes are therefore favorable for application as phosphors and UV–visible energy-converting devices. In another study, flexible luminescent BC/CdSe nanocomposite membranes were fabricated by the *in situ* synthesis of CdSe NPs on the BC nanofibers (Figure 2).[42] The obtained BC/CdSe nanocomposites exhibited improved thermal stability (increment up to 38°C), good photoluminescence (emission peak at 529 nm resulting from the transition of electrons from shallow states near the conduction band to selenium vacancies near the valence band), and excellent mechanical properties (tensile strength = 31.9 MPa; Young's modulus = 325.9 MPa). These flexible and photoluminescent membranes are likewise suitable for application in several fields as sensors and security papers. In a quite different line, Ai et al.[43] prepared water-soluble (at pH 8) and highly luminescent (CdSe)ZnS QDs by using two amino acids, specifically histidine and *N*-acetyl-cysteine, to replace the original organic capping groups of the QDs and successfully assembled them onto bacterial microcrystalline cellulose via cellulose binding proteins. Photoluminescence spectroscopic studies showed that these protein-bound QDs exhibit near-identical photophysical behavior as the unbound counterparts. Meanwhile, the specific binding properties of the proteins onto cellulose have persisted to be active.

Cellulose Derivative-Based Materials

Cellulose derivatives, including ethylcellulose,[44–51] nitrocellulose,[51] hydroxypropylcellulose,[62] cellulose acetate,[52–56] carboxymethylcellulose,[57–61] cellulose acetatebutyrate,[45,46] and cyanoethylcellulose[63] have also been extensively used as solid substrates for the preparation of novel luminescent materials, mainly for the preparation of sensors, because of their specific properties and solubility in several organic solvents.

Ethylcellulose is one of the most used cellulose derivatives in this field because it is stable, nontoxic, and substantially water insoluble. For instance, Volkan et al.[44] developed a novel tubular device for the determination of hydrogen sulfide in air, using several solid substrates, including ethylcellulose, treated with a $CdCl_2$ solution. The analyte reacts with the solid substrate to form a luminescent spot whose length in the tube is measured and correlated to its concentration in the air sample.

The effect of humidity on the sensitivity of luminescent platinum octaethylporphyrin thin film oxygen sensors when hydrophilic polymers, as ethylcellulose and cellulose acetatebutyrate, are used as binding matrix was investigated by Eaton and Douglas.[45] When using ethylcellulose, sensitivity is nearly halved at 85% relative humidity when compared with 0% relative humidity. However, for cellulose acetate butyrate, sensitivity is only reduced by 14% at the same conditions. Time-resolved studies suggest that the effect of humidity lies in changes of the oxygen permeability in the polymer rather than on the distribution of the lumophore sites in the matrix. Later on, this research group also reported a kinetic study on the oxygen quenching of Pt and Pd octaethylporphyrin luminescence in the same polymer films[46] and an artless colorimetric luminescent oxygen sensor using a colored (green) light emission diode with Pt octaethylporphyrin ethylcellulose comprising TiO_2 and ZnO as the oxygen-responsive components.[47] In another study, luminescent dual sensors for time-resolved imaging of pCO_2 and pO_2 in aquatic systems were designed by the incorporation of tris(tetraoctylammonium)-8-hydroxypyrene-1,3,6-trisulfonate acting together with tetraoctylammonium hydrogen carbonate buffer as pCO_2-sensing system along with the oxygen indicator tris(4,7-diphenyl-1,10-phenanthroline)rutheniu-m(II) bis(3-(trimethylsilyl)-1-propanesulfonate) into a single layer

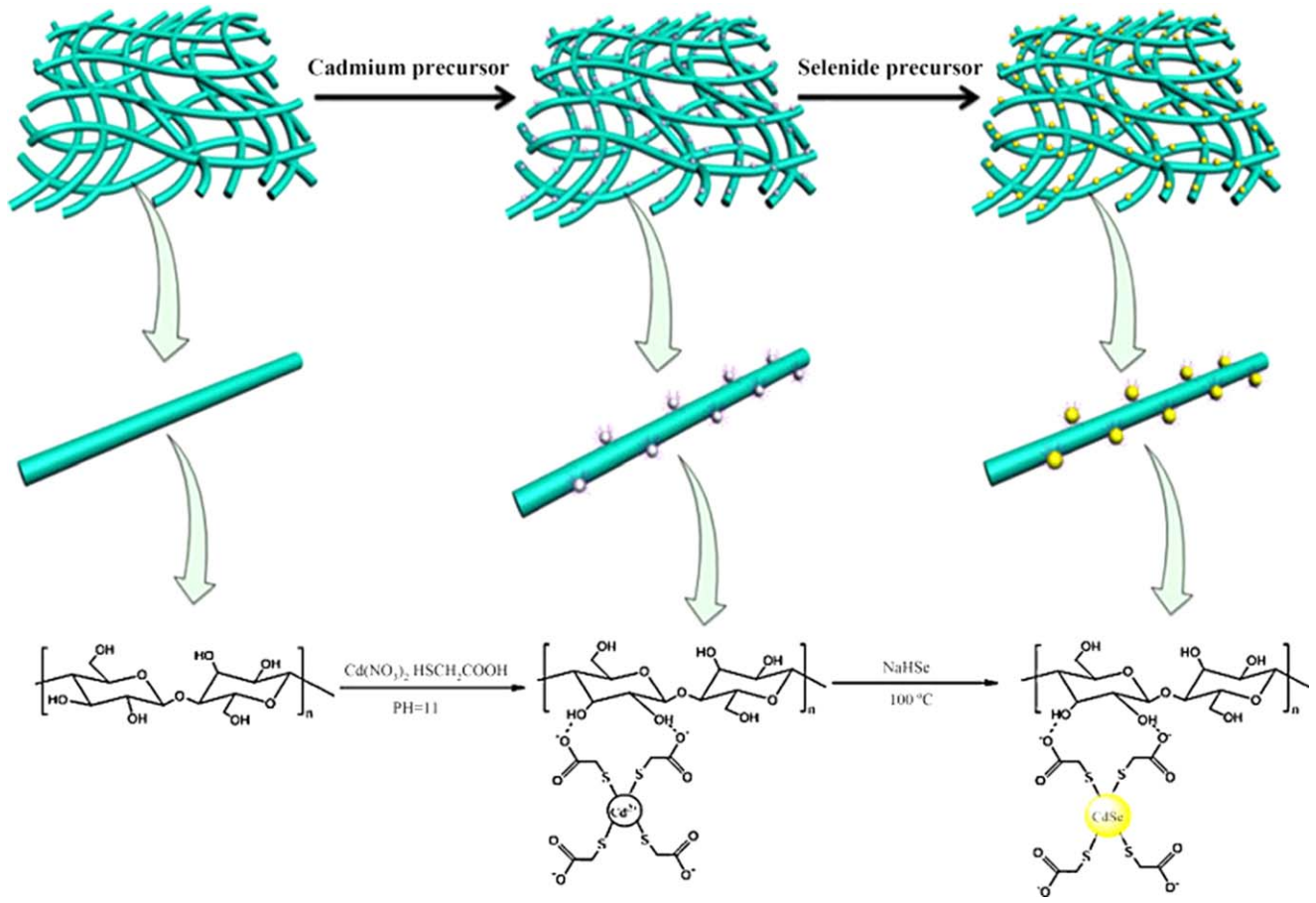

Figure 2. Schematic illustration of the formation of CdSe/bacterial cellulose nanocomposites. (Reproduced from Ref. 42, with permission from Elsevier). [Color figure can be viewed in the online issue, which is available at wileyonlinelibrary.com.]

of ethyl cellulose matrix.[48] The two sensing systems were simultaneously excited at 460 nm, and a fast, gateable charge-coupled device camera was used as the detector. The time-gated imaging scheme enables the simultaneous mapping of pCO_2 and pO_2.

In a different vein, Generalova et al.[49] described the preparation of highly luminescent ethyl cellulose NPs containing embedded semiconductor (CdSe)ZnS QDs. It was observed that the embedding of QDs that yields ethylcellulose NPs resulted in fluorescence intensity twice higher than that of the native QDs nanocrystals. The attained fluorescent ethylcellulose NPs were functionalized by immobilization of a specific antibody and applied in rapid agglutination test for detection of *Yersinia pestis* F1-antigen.

Recently, Achatz et al.[50] described the first sensor for oxygen that can be excited with NIR light. This novel luminescent oxygen sensor is based on a quenchable probe and NPs (NaYF4 : Yb, Tm) incorporated in a thin layer of ethylcellulose. These NPs are used as a kind of nanolamps whose visible emission acts as the light source that is causing photoexcitation of an iridium(III) complex. The fluorescence of this complex, in turn, is dynamically quenched by oxygen. In a complete different vein, two cellulose derivatives, ethylcellulose and nitrocellulose, were used as vehicles to fabricate white-colored pastes from the mixture of Y_2O_3 : Eu (red), $LaPO_4$:Ce, Tb (green), and $BaMgAl_{10}O_{17}$: Eu (blue) for flat fluorescent lamps.[51] The phosphor paste synthesized with nitrocellulose showed superior adhesion behavior, low residual carbon content, and excellent luminescent properties. Similarly, (hydroxypropyl)methyl cellulose was used as an additive to a precursor solution used in the preparation of V_2O_5, Y_2O_3, and YVO_4 as well as luminescent Eu-doped YVO_4 films by spin coating.[62] However, in these two examples, the cellulosic polymers only display a significant role on the preparation of the pastes or the films, because before their usage, the biopolymers are removed by calcination.

Oxygen-sensitive films were prepared using luminescent ruthenium diimine cationic complexes solubilized in a hydrophobic-plasticized polymer medium (specifically cellulose acetate plasticized with tributylphosphate) through ion-pair coupling with a hydrophobic anion (tetraphenyl borate).[52] The luminescence response of the film toward oxygen increased with the level of plasticizer used, and its sensitivity is largely independent of temperature. In a more fundamental vein, Yoshinaga et al.[53] studied the influence of solid surface properties of powders and films on the chemiluminescence characteristics using several polymers (including cellulose and cellulose acetate) as solid

media and a chemiluminescent reagent with a composition similar to that of Cyalume®. The effects of functional groups of the polymers were also inspected.

Surface-modified NPs (about 20 nm) of silicon containing fluorescein isothiocyanate emit strong and stable phosphorescence on cellulose acetate membranes at room temperature.[54] When the primitive color-producing agent in the enzyme-linked immunosorbent assay (ELISA) tools, for determination of alpha-fetoprotein (AFP), was replaced with these luminescent NPs, the system maintained good phosphorescence properties, and the phosphorescence intensity enhanced markedly after the ELISA reaction. Therefore, this methodology represents a new and highly sensitive methodology for the detection of human AFP. In a similar vein, Liu et al.[56] suggested a simple and precise (limit of quantification of about 8.0×10^{-14} g mL^{-1}) immunoassay for the quantification of calcitonin in human serum using water-soluble multiwalled carbon nanotubes (MWCNTs). The COOH group of MWCNTs could react with the NH group of rhodamine S, which could emit room-temperature phosphorescence on cellulose acetate membrane, and react with Tween-80 to form a micellar compound. Recently, Bomm et al.[55] reported on the fabrication and spectroscopic studies of highly luminescent and transparent (>93%) CdSe/CdS nanorods poly(lauryl methacrylate) and cellulose acetate-based composites. A photoluminescence quantum efficiency of 70% and 52% was obtained with 0.05 and 0.5 wt % of CdSe/CdS nanorods, respectively, for poly(lauryl methacrylate) and cellulose acetate. It was found that in the case of cellulose acetate, the nanorods are agglomerated.

Carboxymethylcellulose has also been gaining interest in this research field because of its properties such as high transparency and film-forming ability. For example, Liu et al.[57,58] reported the preparation of luminescent lead carboxymethylcellulose particles containing salycil fluorenones that emit intense and stable phosphorescence on filter paper at room temperature. These particles were successfully used for the determination of trace mercury and silver in water samples by quenching phosphorescence in a linear range of 2.0–40.0 fg $spot^{-1}$ (5.0–100.0 pg mL^{-1}) and 8.0–40.0 fg $spot^{-1}$ (20.0–100.0 pg mL^{-1}) with a detection limit of 0.26 and 2.2 fg $spot^{-1}$, respectively. The room temperature and microwave irradiation synthesis of carboxymethylcellulose/transitions metals (Cu, Ag, and Fe) nanocomposites was described by Nadagouda and Varma.[59] The obtained nanocomposites display wider decomposition temperatures, and the Ag-based nanocomposites also show luminescence at longer wavelengths (green light emission at 365 nm UV radiation source). This environmentally friendly methodology permits the production of numerous fashioned nanostructures without the use of any harmful reagents and therefore could find several potential technological and medicinal applications. Luna-Martínez et al.[60] studied the preparation and optical characterization of ZnS–sodium carboxymethylcellulose films obtained by casting after *in situ* precipitation of ZnS in sodium carboxymethylcellulose aqueous solution. The ensuing nanocomposite films displayed optical transmission between 50 and 90% depending on the amount of ZnS nanocrystals used. The photoluminescence spectra of the nanocomposite films exhibit a broad visible emission band centered at 445 nm (under UV light excitation, $\lambda = 320$ nm) and therefore might have a potential application in security papers by means of an optical signature. Recently, a novel method for the determination of iodate based on carboxymethylcellulose-capped CdS QDs was developed by Tang et al.[61] Under the optimum conditions, the relative fluorescence intensity of CdS QDs was linearly proportional to iodate concentration over the range of 1.0×10^{-8} to 1.0×10^{-5} mol L^{-1} with a correlation coefficient of 0.9987 and a detection limit of 6.0 nmol L^{-1}.

Finally, luminescent composite films were prepared by integration of low-toxic CuInSe QDs into a cyanoethylcellulose[63] matrix following a casting methodology. These films are flexible, showed a high transparency (transmittance up to around 80% at 700 nm), and their emissive color can be tunable over green, yellow, orange, pink, and red by varying the relative amount of QDs. Therefore, this kind of transparent films could find applications in solid-state lighting emission diodes, light-emitting devices, and laser displays.

CHITOSAN-DERIVED LUMINESCENT MATERIALS

Chitosan, obtained by deacetylation of chitin (the second most abundant natural polymer), is a cationic polysaccharide that exhibits unique properties, including biocompatibility, antimicrobial activity, and excellent film-forming ability.[130] In particular, its filmogenic aptitude from acidic aqueous solutions makes it as one of the most attractive biopolymeric substrates regarding the preparation of transparent luminescent bio-based composites. Indeed, chitosan matrices have already been combined with distinct luminescent fillers (including metal complexes, QDs, metal nanostructures (NPs and metal clusters), metal oxides (ZnO), and carbon nanostructures) that retain their luminescent properties or that in some cases even increase their quantum yield. These chitosan-based luminescent materials were firstly used as coatings for electrodes.[64–71] Nevertheless, their preparation in other forms as regular films,[72–75] nanospheres/microspheres,[75–77,79–92] or only as capping agent[78,93–96] have also been reported as strategies to get advanced luminescent bio-based materials for distinct applications.

Chitosan Coatings for Electrodes

The pioneering work using chitosan for the development of luminescent materials was reported by Zhao et al.[64] In this study, chitosan was used to coat a platinum electrode resulting in a membrane film (about 5 μm thickness) around the electrode. The incorporation of Ru(II) complex moieties inside chitosan matrix allowed their use as luminous membranes for the preparation of an electrochemiluminescence (ECL) optic sensor with good sensitivity for the detection of oxalic acid. Recently, Qu et al.[65] and Cai et al.[66] proposed novel approaches to fabricate tris(2,2′-bipyridyl)ruthenium(II) ($Ru(bpy)_3^{2+}$)–chitosan composite coating films for graphite and glassy carbon electrode surfaces, respectively. The introduction of gold NPs, which act as conducting pathways to connect $Ru(bpy)_3^{2+}$ sites to the electrode in the membranes, in the chitosan composite films results in accelerated charge transport through the film and improved inductivity and stability. Similarly, the use of Ru(II) complex-

doped amino-functionalized silica NPs allowed a better binding to the film.[66] These methodologies offered the possibility of producing electrodes with higher sensitivity and long-term stability.

The use of QDs has also emerged as an attractive alternative to traditional fluorescent organic dyes and metal complexes for the preparation of chitosan-based luminescent materials. For example, Zhao et al.[68] developed a sensitive flow-injection analysis system with ECL detection where chitosan was used to immobilize CdTe QDs and CNTs onto indium tin oxide glass electrodes of an anodic sensor. Dopamine was used as model compound to verify the performance of the novel sensor, and a sensitive ECL quenching response within the linear range of 10 p*M* to 4 n*M* and a detection limit of 3.6 p*M* were achieved. This innovative approach was evaluated in two real cerebral spinal fluid samples, with satisfactory results demonstrating the applicability and reliability of this sensor cell.

After verifying the emergence of photoluminescent carbon-based nanomaterials in the search for more "benign materials" (in comparison with QDs) for bioimaging and disease detection, Zhang et al.[67] developed an ECL sensor based on a CNTs–chitosan/AuNPs composite-modified screen-printed carbon electrode and using PtAg@carbon nanocrystals composites as labels. This ECL immunosensor exhibited good stability, amplification effect, and satisfactory analytical performance, with an intensity six times higher than that of pure carbon nanocrystals. It was tested for the sensitive detection of cancer biomarkers; furthermore, its application could be extended to other biomarkers important for accurate clinical disease diagnostics. In a similar line, Jie et al.[69] applied a colloidal solution containing CNTs, QDs, and chitosan to cover an Au electrode surface yielding a robust film with high ECL intensity and good biocompatibility. The subsequent covalent linkage of 3-aminopropyltriethoxysilane to the latter film promoted a considerable enhancement of the ECL (20-fold higher), which was attributed to the simplification of the radical generation and electron-transfer processes due to the presence of amine groups. This modified electrode was successfully applied to the detection of IgG in human serum samples (detection limit was 0.001 ng mL^{-1}) and therefore could be used as an ECL immunosensor.

More current works also showed the possibility of using luminescent graphene–chitosan–based films to modify the surface of electrodes.[70,71] One strategy considered the combination of L-cysteine-capped CdSe QDs with graphene oxide (GO) and chitosan by ultrasonic mixing of all components yielding a composite film with a porous structure where the QDs are dense and homogeneously dispersed.[70] This novel material showed a photoluminescence emission spectrum similar to that of pure QDs, except for a small intensity decrease attributed to the electron transfer from excited QDs to GO–chitosan sheets. Using a glass carbon disk electrode modified with this composite film, it was verified that the ECL intensity is more than 2.5-fold higher than that observed for pure CdSe QDs. Because of the strong and stable ECL emission, this material demonstrates a high sensitivity and good selectivity to cytochrome *c* (linear range from 4 to 324 μM; detection limit of 1.5 μM). In another study, Wu et al.[71] demonstrated the possibility of fabricating an immunosensor by covalent immobilization of captured antibodies on a chitosan/electrochemically reduced GO (RGO) film-modified glass carbon electrode. The purpose of this composite film was to accelerate the electron transfer between the electrode and the QDs-coated silica NPs, which were used as tracing tags to enhance the detection signal. The corresponding identity and amount of the respective antigen were determined as each biorecognition event yields a distinct voltammetric peak with distinct position and size.

Self-Standing Chitosan Films

The possibility of preparing self-standing luminescent chitosan films was explored by different authors as a way to enlarge their applications fields besides the previously described electrode coatings. In particular, taking advantage of their high transparency in the UV–vis region, some works revealed the possibility of preparing chitosan films doped with distinct luminescent fillers through the simple blending of components.[72,73]

For example, Tsvirko et al.[72] prepared chitosan films doped with Eu^{3+} β-diketonate complex, which showed good luminescence emission in the visible region, with a quantum efficiency of $\sim$ 47%. In a different study, Kumar et al.[73] described the preparation of highly luminescent and antibacterial chitosan-based films loaded with water-soluble L-cysteine-functionalized CdTe QDs with a wide-range dispersion of 3–18 nm. It was observed that for the same excitation wavelength, QDs show an emission at 525 nm, whereas CdTe QDs–chitosan film shows an emission at 514 nm; this blue shift was explained based on the electrostatic conjugation of CdTe QDs with L-cysteine. These films can be used as a potential tool in biomedical applications, specifically in terms of tracking the cells and intracellular processes.

George et al.[74] demonstrated the feasibility of using gold nanoclusters in a device arrangement using chitosan as the film matrix (Figure 3). The Au_{15} quantum nanoclusters were encapsulated in a cyclodextrin, aiming to increase both chemical and thermal stability of the clusters, before being dispersed on a dried chitosan film soaked with sodium citrate to enhance the film strength. These multifunctional free-standing films showed abrupt and specific luminescent changes only to Cu^{2+} ions (among other tested metal ions), which is explained by a possible reduction of copper ions by the glutathione ligand or the Au_{15} core. This research group also investigated the possibility of using proteins, namely, lactoferrin, as gold clusters stabilizers.[75] Specifically, native lactoferrin-protected Au clusters were anchored onto GO/RGO substrates through simple electrostatic interaction at nearly neutral pH (6.5) and then mixed with a chitosan solution resulting in a nanocomposite film material after solvent casting. The transparency of the composite can be modulated by controlling the load of RGO/GO. In addition, the obtained films displayed reasonable stability against pH and temperature variations, antibacterial activity, and luminescent properties being therefore promising for bar-coding applications where luminescent patterns can be inscribed and erased by simply wetting of the film.

Chitosan Nanospheres and Microspheres

Chitosan has also been used to fabricate luminescent nanospheres and microspheres, such as chitosan-QDs spheres, where

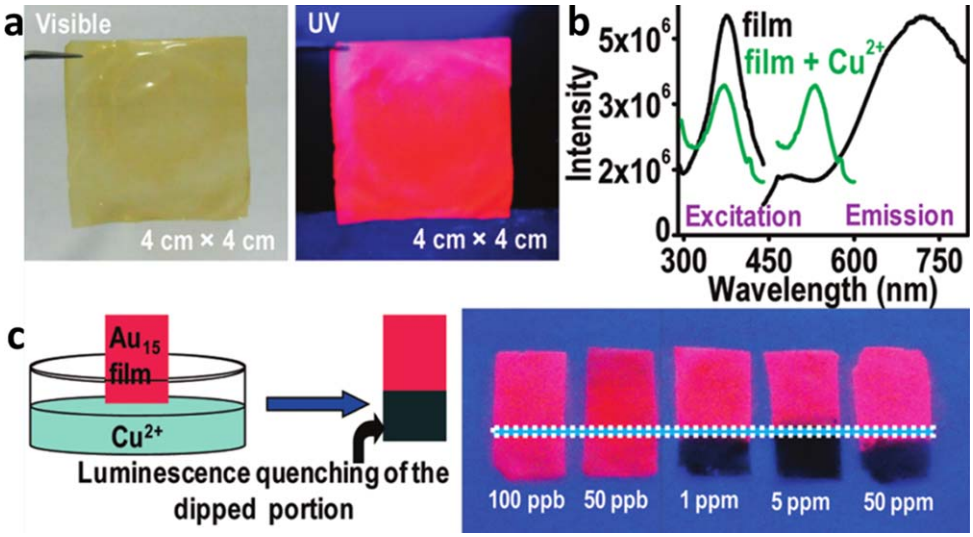

Figure 3. (a) Photographs of the Au nanoclusters incorporated chitosan film under white light and UV light, (b) photoluminescent spectra of the film before and after exposing to Cu^{2+}, and (c) schematic representation of film luminescence quenching and their real visual dependence of Cu^{2+} concentration. (Adapted from Ref. 74, with permission from American Chemical Society). [Color figure can be viewed in the online issue, which is available at wileyonlinelibrary.com.]

chitosan acts simultaneously as the polymeric matrix and stabilizing agent to protect the QDs from fast degradation and oxidation. The first reports on this subject were described by Zhang and coworkers.[76,77] The first work reported a simple method where functionalized QDs (mercaptopropionic acid-capped QDs) were linked to chitosan via reaction of amino groups of chitosan with carboxylic acid groups of QDs.[76] Monodisperse and spherical particles with 102 nm diameter and presenting a quantum yield of 24.7% (11.8% over free QDs) were achieved. This enhancement in the fluorescence emission was explained by the gross electrostatic/polar environment of the inorganic core, which probably affects the efficiency of core electron–hole recombination due to the chitosan encapsulation. Following a similar procedure, these authors also studied the preparation of smaller (60 nm) and more uniform chitosan QDs encapsulated NPs.[77] On average, the NPs were found to contain 34% (by mass) of QDs with an encapsulation efficiency of about 83%. Their fluorescence emission spectra were simply tuned by combination of different multicolored (green and red) QDs on the chitosan NPs. Chitosan/QD NPs remain stable up to pH 9 with no visible sign of agglomeration, and the fluorescence spectra also remained stable over a period of 2 weeks confirming the protection role provided by chitosan. Because of their small size, these NPs were readily internalized into myoblast cells showing their potential application in long-term cell imaging.

Following the main concepts of these ground-breaking works, Zhao et al.[78] developed a turn-on fluorescent lead ion sensor where modified mercaptoacetic acid QDs were capped with chitosan and subsequently functionalized with xylenol orange via LbL self-assembly. The fluorescence of the QDs was quenched by an electron transfer mechanism after xylenol orange was bound to the QDs. Nevertheless, the addition of Pb^{2+} originated a dramatic enhancement of the fluorescence intensity, which resulted from the coordination between Pb^{2+} and xylenol orange and the consequent disruption of the electron transfer mechanism. The linear relationship in the recovery of the fluorescence intensity was applied for the determination of Pb^{2+} in real samples, with the results validated by atomic absorption spectroscopy. It is worth noting that the selectivity of the proposed method was also tested by studying the interfering effect of foreign ions and that only Cu^{2+} showed some interference at a concentration of 1 μmol L^{-1}.

In a distinct study, Chelebaeva et al.[79] designed a straightforward method to prepare ultrasmall (3–4 nm) magnetoluminescent polymer NPs enwrapped by chitosan. This approach is based on an association of luminescent Ln^{3+} and paramagnetic Gd^{3+} ions with paramagnetic octacyanomolybdate building blocks to obtain biocompatible and high-stable NPs, even at low pH. Aqueous colloidal solutions of these NPs showed the luminescence characteristic of the corresponding lanthanides (Eu^{3+} and Tb^{3+}) under UV excitation. An important feature of these NPs was that the nuclear relaxivity r_{1p} is slightly higher (or comparable) than that of commercial magnetic resonance imaging contrast agents, being rapidly internalized *in vitro* by both healthy and living cancer cells. Furthermore, they can be easily detectable in the cells by fluorescence microscopy at extremely low doses (100 ng mL^{-1}).

Another methodology in this topic was presented by Wang et al.,[80] in which water-soluble and biocompatible NPs (around 23 nm) comprising LaF_3 nanocrystals doped with Eu^{3+} were obtained by a coprecipitation method. These NPs showed non-uniform lattice fringes, suggesting that chitosan might be present both on the surface and inside the NPs. These structures were found to be strongly fluorescent and stable in an aqueous solution for a time period of 15 days or in a pH range from 2 to 7.4. Its emission spectrum displayed characteristic emission

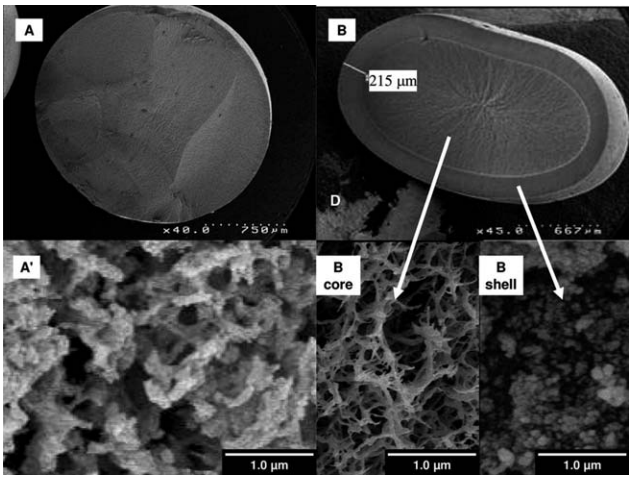

Figure 4. SEM of cross sections of homogeneous (A and A′) and core–shell structure (B). (Reproduced from Ref. 82, with permission from American Chemical Society.)

peaks of Eu^{3+}, from 520 to 720 nm, corresponding to the transitions from the excited $^5D_1$ and $^5D_0$ levels to ^7F_J levels. Moreover, these NPs demonstrated to be biocompatible to human colon HT-29 cells and capable of attaching to bovine serum albumin proteins, probably due to the functional chemical groups provide by chitosan.

Chen et al.[81] also reported an approach to prepare luminescent nanocrystals–chitosan NPs that could be applied in specific targeting and imaging of lung cancer cells. Folic acid–chitosan chemically coupled conjugates were successfully used for the surface functionalization of $NaYF_4$: Yb/Er nanocrystals, as confirmed by FTIR analysis, by the simple mixing of all components. Folic acid was used because of the high affinity of folate moieties to receptors, being suitable for targeting cell membrane and internalizing into the cell through the receptor-mediated endocytosis, even when conjugated with a wide variety of molecules. Well-dispersed NPs with an irregular spherical shape, no apparent aggregation, and an average diameter of 28 nm were obtained. These NPs demonstrated specific targeting imaging for H460 lung cancer cells; however, nontargeted imaging was observed in human lung fibroblast cells. Therefore, these low cytotoxic conjugates can provide a powerful platform for early diagnosis of lung cancer.

Taking advantage of the versatility of sol–gel processes, Liu et al.[82] developed a refined methodology to prepare chitosan–silica hybrids containing Ln^{3+} (Figure 4). First, chitosan aerogel beads were obtained by drying of alcogel spheres under supercritical CO_2 conditions. The silica incorporation was achieved by two distinct procedures, namely, by condensation (homogeneous structure) and by aggregation of the particles when the alcogel spheres of chitosan are reacted with Ludox® colloidal silica (core–shell structure), aiming to obtain different microstructures. However, the postsynthesis treatment proved to be the most effective. In the core–shell hybrids, the Eu^{3+} probe resides essentially in the chitosan core, whereas the Si content is restricted to the shell. The large number of coordinated hydroxyl groups in both environments results in similar $^5D_0$ quantum efficiency values (4–6%), independently of the structure of the materials.

A fully different methodology was proposed by Yan et al.[83] where using *N,N′*-methylenebis(acrylamide) as crosslinking agent and potassium persulfate as initiator, europium was incorporated on chitosan by free radical and grafted copolymerization. This procedure allows obtaining a red, homogeneous, transparent, and luminescent hydrogel that showed stronger strength fluorescence emission at 615 nm.

Silver nanoclusters were also used to prepare 80 nm spherical hybrid nanospheres based on a nonsolvent aided counter ion complexation method.[84] Specifically, chitosan was mixed with EDTA and the obtained solution was blended with Ag^+, then sodium borohydride was added to reduce silver ions, and finally, glutaraldehyde was added as crosslinking agent. These hybrid nanospheres showed yellowish fluorescence under 365 nm radiation, with an emission centered at 562 nm and an estimated quantum yield of $\sim$ 0.9% demonstrating a high potential as bioimaging agents.

Shen et al.[85,86] reported the preparation of spherical luminescent/magnetic hybrid NPs by direct gelation of chitosan with CdTe QDs and superparamagnetic iron oxide (Fe_3O_4). The inorganic fillers stay randomly distributed all over the hybrid NPs with the morphology and properties strongly dependent on components feeding ratios and the sizes on temperature, pH, NaCl concentration, and reaction time. These magnetic and fluorescent hybrid NPs were further used for insulin loading and therefore can be applied as a targeting carrier for insulin delivery, cell imaging, and antidiabetic investigation of dietary supplements.[85] Additionally, by conjugation with folate tetrapeptide composites, they could be successfully trapped in tumor tissues, even in tumor cells under external magnetic field guidance.[86] Following a different approach, Guo et al.[87] also prepared magnetic/luminescent hybrid microspheres with CdTe QDs/iron oxide NPs cores and chitosan–poly(methacrylic acid) shells. Such hybrid microspheres have uniform size distribution (pH range 5.0–11.0), multiple CdTe cores with controlled magnetic content, and unique pH-responsive reversible fluorescence emission between pH 7.0 and 4.0. Preliminary tests proved that a short time (0.5 h) of exposure to a magnetic field improved the uptake efficiency of the microspheres, whereas a longer time contributed to the cell (liver PLC/PRF/5 cells) death as excess particles have a negative effect on the cell viability or growth.

Sandros et al.[88] and Deng et al.[89] reported interesting less toxic alternatives to prepare fluorescent chitosan nanospheres based on III–V and quaternary alloy Zn–I–III–VI QDs, respectively. In the first case, InGaP QDs overcoated with several monolayers of ZnS were covalently bound to chitosan by a simple blending of components, yielding 29 ± 11 nm composite nanospheres. The QDs were further activated by the addition of 1-ethyl-3-(3-dimethylamino-propyl)carbodiimide hydrochloride producing noncytotoxic and long-wavelength emitting fluorescent probes. A combination of *in vitro* and *in vivo* trials revealed that chitosan not only functioned as a protective barrier to decrease oxidation but also improved cellular uptake drastically. Deng et al.[89] reported a one-pot approach to prepare oil-soluble and

highly luminescent quaternary alloy Zn–Ag–In–Se QDs, using monomeric cyclic arginylglycylaspartic acid (RGD) peptide-modified chitosan-based micelles. These low cytotoxic oil-soluble quaternary QDs kept the shape, crystal structure, and optical properties of the initial QDs and showed a bright photoluminescent emission (quantum yield of close to 50%), as well as a widely tunable maximum in the region from 660 to 800 nm. Their potential as versatile fluorescent probes for *in vitro* and *in vivo* optical imaging was confirmed by optical imaging techniques.

Another promising alternative to obtain "cadmium-free" materials explored the use of zinc-based compounds because of their natural environmental abundance and potential nontoxicity. In this sense, Ramanery et al.[90] capped ZnS QDs with chitosan using a facile, single-step aqueous processing methodology, at room temperature and in aqueous medium. ZnS QDs–chitosan NPs with size diameters between 3.8 and 4.7 nm were obtained, with the ZnS conjugates stabilized by the functional groups of chitosan. Furthermore, the possible tuning, by adjusting the pH, influence their optical fluorescent behavior, which was assigned to the "trap states" emissions involving the defect states of the QDs. These luminescent-tuned NPs present a great potential for use in biomedical and eco-friendly applications; however, further studies are imperative to fully address these issues. Some other authors also tried to dope ZnS QDs with manganese[91] to passivate the ZnS and consequently its high luminescence. These ZnS : Mn^{2+} QDs were synthesized by simple mixing of zinc and manganese acetate and subsequent biofunctionalization with chitosan. The 7 nm QDs encapsulated with chitosan were obtained and attached to the anionic cell wall of *Escherichia coli* bacteria. Photoluminescence spectroscopy studies showed that when attached to bacteria, a distinct blue shift from 590 nm (orange) to 520 nm (green) in the characteristic peak was observed. This feature demonstrated the possible use of these nanostructures as biosensors to detect the presence of bacteria in water and other contaminated samples.

The use of ZnO-based nanocomposites as luminescent tags for cellulosic materials and suitable for use as printed security materials was described by Saeed et al.[92] Specifically, chitosan–ZnO nanospheres and chitosan–ZnO–oleic acid QDs were obtained. These novel ZnO nanocomposites showed distinct photoluminescent emissions bands at $\sim$ 420 nm attributed to the interstitial oxygen, at 485 nm probably originated by the electron transition from the ionized oxygen vacancies level to the valence band, and at $\sim$ 530 nm related to the deep level. Chitosan–ZnO–oleic acid : Eu^{3+} nanorods, which showed an enhanced intensity despite a small red shift (20 nm), were also prepared by doping with an europium salt.

Moreover, other authors also used chitosan as capping agent for silver NPs,[93] Ni_3Se_2 NPs,[94] gold nanorods,[95] or even CdS QDs.[96] However, in these cases, chitosan acts mainly as stabilizer being normally used to improve the biocompatibility of the nanostructures retaining their luminescent properties.

Chitosan Derivatives

As described for cellulose, chitosan derivatives, namely, carboxymethyl chitosan[97–99] and a water-soluble derivative,[100,101] have also been used in the development of new luminescent materials mainly because of potential improvements on the biocompatibility and stability of the final materials. For example, Li and Wang[97] reported the production of NaYF4 : $Yb^{3+}/Tm^{3+}/Er^{3+}$ nanocrystals via a simple and mild hydrothermal process and by using carboxymethylchitosan as a coating agent. This one-pot strategy allowed the preparation of water-dispersible and biocompatible luminescent NPs. When QDs, with CdTe[98] and CdSe[99] cores, were used for the preparation of fluorescent probes with this chitosan derivative, the methodology used was based on the assembly of the components via chelation of amino and carboxyl groups in carboxymethyl chitosan with QDs. The modified QDs showed improved stability (from 4 months to more than 10 months at room temperature), good dispersivity (narrowly distributed in size [3.5 or 5 nm]),[98,99] and excellent fluorescence properties.

The molecular structure of chitosan derivatives also showed to have a large influence on the optical and crystalline properties of QD-based nanocomposites obtained when a water-soluble chitosan derivative was used.[100] NPs with average size of 3–5 nm were obtained, with their size and the photoluminescence intensity controlled through altering the concentration of the precursor ions and stabilizer solution, the molar ratio of metal ions/$[S^{2-}]$, and refluxing time. Pinto et al.[101] described an interesting approach to obtain polysaccharide-based composite films containing lanthanopolyoxometalates (LnPOMs) using a simple casting methodology. The obtained films were completely transparent and display an emission in the visible spectral range resulting from overlap of the $^5D_0 \rightarrow {}^7F_{0-4}$ Eu^{3+} red emission with the intrinsic polysaccharide emission in the blue/green spectral region. The authors also tested the application of this methodology to other LnPOMs (Eu@SiO_2 and Tb40) and other biopolymers (pullulan) with similar results.

Nevertheless, it is important to highlight that the work made with chitosan derivatives is still very limited and there is plenty of scope to be explored. For example, the use of derivatives with distinct substitution degrees, the use of other derivatives, and/or introduction of several groups are some hypotheses that could simultaneously increase the stability and mechanical properties of the final materials as well as the interaction with the cells.

OTHER BIOPOLYMER-DERIVED LUMINESCENT MATERIALS

Gelatin

Gleitsmann et al.[102] prepared nanocomposite-based gelatin thin films with Ag_2O NPs by casting. Silver nanoclusters were then generated by femtosecond-laser-induced reduction of Ag_2O NPs. The laser-activated area showed light emission values, which considerably exceeded the luminescence intensity of similarly activated simple silver oxide NP films. It was found that the size of the silver nanoclusters depended on the laser exposure time, ultimately leading to the formation of metallic silver areas in the nanocomposite matrix. The materials showed very favorable mechanical properties and long-time stability of the luminescent structures in the matrix, pointing out to possible applications as light-emitting materials for all-optical logic devices or data-storage media. Furthermore, the increased stability

of the luminescent clusters by interaction with the gelatin matrix also call attention to the possibility of gelatin-encapsulated silver clusters as promising biocompatible luminescent sensors for biomedical applications.

Kim et al.[103] described the preparation of gelatin-based nanocomposite films with homogeneously dispersed SWCNTs, compatibilized by using sodium docecylsulfate (SDS). The mechanical stretching of the film induced a substantial uniaxial alignment and isolation of individual SWCNTs, which in turn yields a material with a highly polarized absorption and photoluminescence. The optical absorption spectra of the SWCNT/SDS/gelatin gels showed a series of sharp peaks that are assigned to optical transitions between van Hove singularities in the valence and conduction bands of various SWCNTs. This observation strongly supports the proposal that individual SWCNTs are well isolated in the gelatin matrix, opening the door for new applications in optoelectronics materials.

In another study, Borkovska et al.[104] developed nanocomposite gelatin films with CdSe QDs by reaction of Na_2SeSO_3 with $CdCl_2$ in a gelatin aqueous solution, followed by passivation with ZnS and film casting, yielding films of $\sim$ 0.19 mm thickness, followed by annealing in air at 100°C. The process yielded CdSe QDs with a size of about 3 nm as demonstrated by X-ray diffraction. The thermal annealing of the QDs resulted in a red shift of the PLE and PL bands as well as in changes in the temperature dependence of the PL intensity. These effects are attributed to the cleavage of the surface interactions between Cd atoms and the functional groups of gelatin molecules, which was demonstrated by the fact that on passivation of the QDs with a ZnS shell, the observed effects are substantially reduced.

Raevskaya et al.[105] prepared gelatin films containing CdSe NPs passivated or not with CdS or ZnS. The absorption spectra of nonpassivated CdSe NPs with a first maximum at 2.49 eV (498 nm) point out to average diameters of 2.6 ± 0.3 nm. With the CdS and ZnS passivation, a shift to lower energies, namely, 2.470–2.410 eV or 2.408–2.398 eV, respectively, were observed depending on the CdSe/CdS and CdSe : ZnS ratios. For the photoluminescence, there was a shift from 2.250 eV in pure CdSe NPs to lower energies, that is, 2.238–2.183 eV and 2.179–2.157 eV for NPs passivated with different ratios of CdS and ZnS, respectively. These shifts are explained by partial tunneling of electron wave function into the shells formed. Furthermore, passivation increased photoluminescence intensity by a factor ranging between 1.4–1.8 and 0.3–4.4 for NPs passivated with different ratios of CdS and ZnS, respectively.

The effect of 5 nm Ag NPs in the luminescence of a 10-μm-thick gelatin film activated with rodhamine has been investigated by Efendiev et al.[106] The obtained results demonstrated that the doping of the gelatin films with silver NPs leads to an increase in the intensity of the absorption spectrum by a factor of 1.17 and a short-wavelength shift ($\sim$ 1.5 nm), whereas the intensity of the fluorescence spectrum increases by a factor of $\sim$ 2. This increment is due to spectral overlap between the absorption bands of rhodamine and silver NPs. Light scattered by the NPs is reabsorbed by the rhodamine 6G molecules, increasing the amount of absorbed light. These materials may find applications in miniaturized light-emitting biosensors.

In a complete distinct vein, nanocomposite fibers were prepared by electrospinning using poly(ε-caprolactone) and gelatin containing upconversion uniform and monodisperse NPs of luminescent $NaYF_4 : Yb^{3+}$ Er^{3+} encapsulated in mesoporous silica shells by a core/shell approach.[107] The encapsulated NPs were further loaded with a drug, doxorubicin, and a second one, indomethacin, was loaded on the polymeric matrix. The hybrid nanocomposite material was tested as a drug delivery system, indicating that both drugs released from the electrospun composite fibers with distinct profiles. Indomethacin presented a fast-release profile, whereas doxorubicin showed sustained release behavior. Furthermore, the upconversion NPs luminescent intensity ratios of $^2H_{11/2}/^4S_{3/2}$–$^4I_{15/2}$ to $^4F_{9/2}$–$^4I_{15/2}$ from Er^{3+} vary with the doxorubicin content in the NPs and therefore can be used as sensor for the release of the drug.

Gelatin has also been used in the sol–gel synthesis and/or coating of CdTe[108–111] and CdSe[109] QDs and CdSe/HgSe and CdSe/Ag_2Se core/shell[113] as well as CdS[112] and gold nanoclusters[114] for optical applications. Furthermore, gelatin has also been used as the reactant and structure-directing agent in the hydrothermal synthesis of apple-like Eu^{3+} and Tb^{3+} codoped $LaCO_3OH$ hierarchical nanostructures with tunable white light emission.[115] Although in these cases, we are not dealing specifically with materials where gelatin plays the role of a matrix in a nanocomposite material, this approach might be quite promising notable to improve the biocompatibility of such particles, while retaining the core optical properties in biomedical applications, namely, in the imaging field. Finally, gelatin has also been used as starting material for the hydrothermal preparation of highly fluorescent carbon QDs.[116]

Starch

To the best of our knowledge, the preparation of photoluminescent materials based on starch is limited to a study by Guan and Su.,[117] who reported the preparation of a starch-based material, grafted with a fluorescein derivative, and showed an absorptivity and emission comparable with that of fluorescein ($\lambda_{exc} = 490$ nm; $\lambda_{em} = 515$ nm), with a much lower quantum yield ($\Phi \sim 0.28$ for the starch against $\Phi \sim 0.93$ for fluorescein). It was demonstrated that the florescence of the starch–fluorescein derivative showed a linear response to temperature in the range of 0–60°C and a nonlinear response to pH in the range of 0−12 showing additionally better long-term stability and fast equilibrium response, therefore having the potential as cheap materials for measuring pH and temperature in biological systems.

Additionally, a cationic starch has been reported as part of a complex mixture of polyelectrolytes used to prepare multicolor blue, green, red, and full color films based on semiconductor QDs of ZnSe and CdTe following a LbL approach.[118] However, given the complex nature of the mixture, one cannot assume that starch plays a central role in the properties of the material.

Apart from the mentioned studies, starch has also been used as complexing agent on the sol–gel preparation of nanosized particles of itrium orthovanadate doped with disprosium and with samarium cations,[119] with potential applications as phosphors in high-definition flat displays as well as in the preparation of

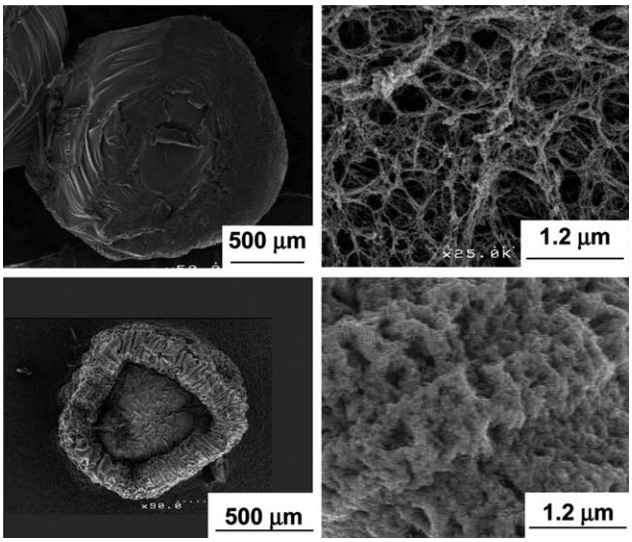

Figure 5. Cross-section micrograph of Eu^{3+}–alginate aerogel (top) and xerogel (bottom). (Reproduced from Ref. 125, with permission from American Chemical Society.)

photoluminescent ZnO[120,121] or CdSe[122,123] NPs. Starch is demonstrated to play a key role as a template for NPs stabilization and to avoid aggregation; however, in the end of the procedures, it was removed either by calcination[119] or by washing[120–123] and therefore did not play any active role in the final optical properties of the final material.

DNA

Leones et al.[124] reported the preparation of a DNA–europium triflate luminescent membrane. Transparent light brown membranes with distinct percentages of the europium salt were prepared, and the resulting materials were shown to be predominantly amorphous and conducive (with the highest values reaching 1.55 mS cm^{-1}). The photoluminescence profile of the DNA–europium membranes showed curves which were well described by a single exponential function, suggesting that on average, Eu^{3+} occupied the same local environment. These materials were studied aiming at applications in solid-state electroluminescent devices and its potential applications.

Alginate

Alginates (polysaccharides produced by brown algae, which are block copolymers of 1 → 4 linked β-D-mannuronic and α-L-guluronic residues, and have a high tendency to form gels with divalent and trivalent cations) have been studied to prepare luminescent hybrid materials containing lanthanide ions (Figure 5)[125] and magnetic/luminescent materials based on CdS and CdTe.[126,127] Photoluminescent alginate aerogels containing Eu^{3+}, Tb^{3+}, Tb^{3+}/Eu^{3+}, and an alginate Eu^{3+} xerogel were prepared by dropping sodium alginate in the trivalent metal solution, forming stable gel spheres; alcogel was then obtained by solvent exchange by immersion of the hydrogel in ethanol with a substantial volume reduction ($\sim$ 20%); and finally, the solvent can be removed by air drying, forming a xerogel, with a drastic volume decrease, producing a dense material, or by supercritical CO_2 drying, forming an aerogel, which results in volume preservation and an open network of fibrils with 10–15 nm in diameter (aerogel).[125] The Eu^{3+}–alginate aerogel and alcogel showed the highest $^5D_0$ quantum efficiencies, whereas the hydrogel and xerogel have lower values (9.9 and 8.2% against 5.2 and 5.6%, respectively). The Tb^{3+}/Eu^{3+} hybrids are multiwavelength emitters in which the emission color can be tuned across the chromaticity diagram from the red toward the yellowish green spectral regions.

In a different vein, highly magnetic luminescent alginate-templated composite microparticles were successfully synthesized by a novel process combining emulsification and LbL self-assembly techniques.[127] The composite microparticles were characterized by ζ-potential analyzer, transmission electron microscope (TEM), XRD, FTIR, fluorescence spectrophotometer, and vibrating sample magnetometer. Experimental observations indicated that the composite microparticles had excellent magnetic properties, and its photoluminescence could be precisely controlled by varying the number of deposition cycles of polyelectrolytes and CdTe/polyelectrolyte multilayers. Moreover, the composite microparticles could be heated up in a high-frequency magnetic field and demonstrated linear temperature-dependent photoluminescence over the range from room temperature to hyperthermia temperature. The composite microparticles are expected to be promising candidates for biomedical applications, such as immunoassay, biosensing and imaging, and cancer diagnosis and treatment.

Finally, sodium alginate as well as a graft copolymer with poly(2-dimethylaminoethyl methacrylate) (PDMA) was also used to passivate the surface of colloidal CdS–thyoglycerol QDs. The surface interaction of the CdS QDs with alginate-*g*-PDMA was assigned to its multidentate ligand character. The resulting passivated QDs showed enhanced emission properties.[126]

Carrageenan

Carrageenans, sulfated polysaccharides extracted from red algae, present a coil–helix transition and helix aggregation dependence on the type and concentration of counter ions that have been explored by Ramos et al.[128] In this study, the authors focus their attention on a mixed valence counter ion system: Eu^{3+}/Na^+ or K^+ with different gel-forming carrageenans: kappa, iota, and kappa-2. The results of stationary and time-dependent luminescence showed to be a suitable tool to probe ion binding to both the negatively charged sulfate group and the hydroxyl groups present in the biopolymer. For lower europium ion concentrations, a single, longer decay emission lifetime was detected, which was attributed to the binding of europium ion to the carrageenan sulfate groups. An additional decay ascribed to europium binding to hydroxyl groups was observed above a threshold concentration, and this decay was dependent on the carrageenan charge density. Symmetry of the europium ion microenvironment was estimated by the ratio between the intensities of its emission bands, which has been shown to depend on the concentration of europium ions and on the specificity of the monovalent counterion bound to the carrageenan.

Dextrin

Finally, Luz et al.[129] prepared luminescent microspheres of a europium(III) dipicolinic acid complex ($[Eu(dpa)_3]^{3-}$) loaded in dextrin (a low-molecular-weight α-(1,4)-glucan) by ultrasonic spray drying, yielding spherically shaped microspheres with a size distribution of 0.6 ± 0.3 μm. The luminescence spectra of the

encapsulated material demonstrated that Eu^{3+} ions emit via ligand excitation at the $\pi \rightarrow \pi^{\star}$ transition (280 nm) followed by an energy intramolecular transfer to the Eu^{3+} excited levels, thus enhancing the red emission (antenna effect). Additionally, the intensity of the luminescent signal is orders of magnitude stronger than that observed for direct excitation of the Eu^{3+} ion. The luminescence spectra before and after the microspheres loading demonstrate that the ultrasonic spray drying process does not change the structure of the $[Eu(dpa)_3]^{3-}$ complex and that emission lifetime and quantum efficiency were only slightly lower after microencapsulation. Thus, the encapsulation promotes the formation of a protective barrier around the photoactive material that might protect it from deterioration, and turns it easy to manipulate.

CONCLUSIONS AND FUTURE PERSPECTIVES

Biopolymers, as polysaccharides, are unique raw materials for the design and development of sustainable functional materials, including luminescent materials as unquestionably corroborated by the extent and assortment of the research activities described in the current appraisal, mainly because of their abundance, diversity, and specific properties.

Among the vast array of potential applications of biopolymer-based composites, the production of novel luminescent bio-based materials for several applications, including optical and electronic devices, biosensors (and other sensors), bioimaging, and drug delivery, has been a matter of intense investigation in recent years. Depending on the nature and characteristic of the biopolymers, as well as of the luminescent fillers, materials can be obtained in distinct forms such as (nano)fibers, self-standing films, coating films (for devices as electrodes or for nanoentities like QDs), and aerogels.

Notwithstanding the enormous use of biopolymers as components of luminescent-based materials, there are still plenty of opportunities to be explored and important advances could be foreseen. One important issue is associated with the environmental impact of some luminescent fillers as well as of the processing methodologies used. For example, QDs composed of Group II and VI metals display recognized cytotoxic effects because of their ability to penetrate into tissues and to release heavy metals like cadmium, lead, and selenium, even after coating with appropriated layers. Therefore, the development of more environmentally friendly luminescent fillers is imperative when considering the use of biopolymers (or even any other polymeric substrate). These progresses must be complemented by the use of green solvent systems (as aqueous and ionic liquid systems) on the preparation and processing of the materials.

Finally, the combination of luminescent fillers with emerging biopolymeric materials (e.g., other bio-based nanofibers and nanocrystals and proteins) will open the opportunity for the development of ground-breaking luminescent materials for a wider sort of applications.

ACKNOWLEDGMENTS

R. J. B. Pinto thanks the Portuguese Foundation for Science and Technology (FCT; Grant no. FRH/BPD/89982/2012) for financial support. C. S. R. Freire and P. A. A. P. Marques also acknowledge FCT for the research grants under the program Investigador FCT 2012 and 2013, respectively. The authors also acknowledge FCT for CICECO (PEst-C/CTM/LA0011/2013; FCOMP-01-0124-FEDER-037271) and TEMA-NRD (PEst-C/EME/UI0481/2013) funding.

REFERENCES

1. Vilela, C.; Cruciani, L.; Silvestre, A. J. D.; Gandini, A. *RSC Adv.* **2012**, *2*, 2966.
2. Vilela, C.; Silvestre, A. J. D.; Meier, M. A. R. *Macromol. Chem. Phys.* **2012**, *213*, 2220.
3. Sousa, A. F.; Matos, M.; Freire, C. S. R.; Silvestre, A. J. D.; Coelho, J. F. *J. Polymer* **2013**, *54*, 513.
4. Vilela, C.; Sousa, A. F.; Freire, C. S. R.; Silvestre, A. J. D.; Pascoal Neto, C. *Biomass Bioenergy* **2013**, *55*, 148.
5. Tomé, L. C.; Pinto, R. J. B.; Trovatti, E.; Freire, C. S. R.; Silvestre, A. J. D.; Neto, C. P.; Gandini, A. *Green Chem.* **2011**, *13*, 419.
6. Fernandes, S. C. M.; Oliveira, L.; Freire, C. S. R.; Silvestre, A. J. D.; Neto, C. P.; Gandini, A.; Desbriéres, J. *Green Chem.* **2009**, *11*, 2023.
7. Figueiredo, A. G. P. R.; Figueiredo, A. R. P.; Alonso-Varona, A.; Fernandes, S. C. M.; Palomares, T.; Rubio-Azpeitia, E.; Barros-Timmons, A.; Silvestre, A. J. D.; Pascoal Neto, C.; Freire, C. S. R. *Biomed Res. Int.* **2013**, 2013, 698141.
8. Pinto, R. J. B.; Marques, P. A. A. P.; Martins, M. A.; Neto, C. P.; Trindade, T. *J. Colloid Interface Sci.* **2007**, *312*, 506.
9. Pinto, R. J. B.; Marques, P. A. A. P.; Neto, C. P.; Trindade, T.; Daina, S.; Sadocco, P. *Acta Biomater.* **2009**, *5*, 2279.
10. Pinto, R. J. B.; Neves, M. C.; Neto, C. P.; Trindade, T. *Eur. J. Inorg. Chem.* **2012**, 2012, 5043.
11. Goncalves, G.; Marques, P. A. A. P.; Pinto, R. J. B.; Trindade, T.; Neto, C. P. *Compos. Sci. Technol.* **2009**, *69*, 1051.
12. Neves, M. C.; Freire, C. S. R.; Costa, B. F. O.; Neto, C. P.; Trindade, T. *Cellulose* **2013**, *20*, 861.
13. Pinto, R.; Marques, P.; Barros-Timmons, A.; Trindade, T.; Neto, C. *Compos. Sci. Technol.* **2008**, *68*, 1088.
14. Binnemans, K. *Chem. Rev.* **2009**, *109*, 4283.
15. Carlos, L. D.; Ferreira, R. A. S.; Bermudez, V. Z.; Ribeiro, S. J. L. *Adv. Mater.* **2009**, *21*, 509.
16. Carlos, L. D.; Ferreira, R. A. S.; Bermudez, V. Z.; Julián-López, B.; Escribano, P. *Chem. Soc. Rev.* **2011**, *40*, 536.
17. Sanchez, C.; Belleville, P.; Popall, M.; Nicole, L. *Chem. Soc. Rev.* **2011**, *40*, 696.
18. Kitai, A., Ed. Luminescent Materials and Applications; Wiley, The Atrium, Southern Gate, Chichester, **2008**.
19. Blasse, G.; Grabmaier, B. C. Luminescent Materials; Springer: Berlin, **1994**.
20. Hänninen, P.; Härmä, H., Eds. Lanthanide Luminescence: Photophysical, Analytical and Biological Aspects; Springer-Verlag, Berlin, Heidelberg, **2011**.
21. Hull, R.; Parisi, J.; Osgood, R. M.; Warlimont, H.; Liu, G.; Jacquier, B., Eds. Spectroscopic Properties of Rare Earths

in Optical Materials, Springer-Verlag, Berlin, Heidelberg, **2005**.

22. Ferreira, L. F. V.; Netto-Ferreira, J. C.; Khmelinskii, S. I. V.; Garcia, A. R.; Costa, S. M. B. *Langmuir* **1995**, *11*, 231.
23. Ilharco, L. M.; Garcia, A. R.; DaSilva, J. L.; Lemos, M. J.; Ferreira, L. F. V. *Langmuir* **1997**, *13*, 3787.
24. Ferreira, L. F. V.; Lemos, M. J.; Reis, M. J.; do Rego, A. M. B. *Langmuir* **2000**, *16*, 5673.
25. Habibagahi, A.; Mébarki, Y.; Sultan, Y.; Yap, G. P. A.; Crutchley, R. *J. ACS Appl. Mater. Interfaces* **2009**, *1*, 1785.
26. Small, A. C.; Johnston, J. H. *Curr. Appl. Phys.* **2008**, *8*, 512.
27. Kim, H.; Petryayeva, E.; Algar, W. R. *J. Quantum Electron.* **2014**, *20*, 7300211.
28. Niu, T.; Gu, Y.; Huang, J. *J. Mater. Chem.* **2011**, *21*, 651.
29. Zhang, Y.; Huang, J. *J. Mater. Chem.* **2011**, *21*, 7161.
30. Kulpinski, P.; Erdman, A.; Namyslak, M.; Fidelus, J. D. *Cellulose* **2012**, *19*, 1259.
31. Kulpinski, P.; Namyslak, M.; Grzyb, T.; Lis, S. *Cellulose* **2012**, *19*, 1271.
32. Chang, C.; Peng, J.; Zhang, L.; Pang, D.-W. *J. Mater. Chem.* **2009**, *19*, 7771.
33. Zhou, Z.; Wang, Q. *Sens. Actuator B* **2012**, *173*, 833.
34. Tan, C.; Wang, Q. *J. Fluoresc.* **2012**, *22*, 1581.
35. Huo, J.; Zheng, Y.; Pang, S.; Wang, Q. *Cellulose* **2013**, *20*, 841.
36. Wang, Q.; Zhang, Z.; Zheng, Y.; Cai, W.; Yu, Y. *CrystEngComm* **2012**, *14*, 4786.
37. Van Opdenbosch, D.; Maisch, P.; Fritz-Popovski, G.; Paris, O.; Zollfrank, C. *Carbohydr. Polym.* **2012**, *87*, 257.
38. Olivier, C.; Moreau, C.; Bertoncini, P.; Bizot, H.; Chauvet, O.; Cathala, B. *Langmuir* **2012**, *28*, 12463.
39. Pikulev, V. B.; Loginova, S. V.; Gurtov, V. A. *Tech. Phys. Lett.* **2012**, *38*, 723.
40. Díez, I.; Eronen, P.; Österberg, M.; Linder, M. B.; Ikkala, O.; Ras, R. H. A. *Macromol. Biosci.* **2011**, *11*, 1185.
41. Caiut, J. M. A.; Barud, H. S.; Santos, M. V.; Oliveira, U. L.; Menezes, J. F. S.; Messaddeq, Y.; Ribeiro, S. J. L. In Martín-Palma, R. J.; Jen, Y.-J.; Mackay, T. G., Eds.; Luminescent multifunctional biocellulose membranes, Society of Photo-Optical Instrumentation Engineers (SPIE), San Diego, **2011**; Vol. *8104*, pp 81040Z-1-81040Z-9.
42. Yang, Z.; Chen, S.; Hu, W.; Yin, N.; Zhang, W.; Xiang, C.; Wang, H. *Carbohydr. Polym.* **2012**, *88*, 173.
43. Ai, X.; Xu, Q.; Jones, M.; Song, Q.; Ding, S.; Ellingson, R. J.; Himmel, M.; Rumbles, G. *Photochem. Photobiol. Sci.* **2007**, *6*, 1027.
44. Volkan, M.; Eroglu, T.; Eroglu, A. E.; Ataman, O. Y.; Mark, H. B. *Talanta* **1998**, *47*, 585.
45. Eaton, K.; Douglas, P. *Sens. Actuator B* **2002**, *82*, 94.
46. Eaton, K.; Douglas, B.; Douglas, P. *Sens. Actuator B* **2004**, *97*, 2.
47. Ricketts, S. R.; Douglas, P. *Sens. Actuator B* **2008**, *135*, 46.
48. Schroeder, C. R.; Neurauter, G.; Klimant, I. *Microchim. Acta* **2007**, *158*, 205.
49. Generalova, A. N.; Sizova, S. V.; Oleinikov, V. A.; Zubov, V. P.; Artemyev, M. V.; Spernath, L.; Kamyshny, A.; Magdassi, S. *Colloids Surf. A* **2009**, *342*, 59.
50. Achatz, D. E.; Meier, R. J.; Fischer, L. H.; Wolfbeis, O. S. *Angew. Chem. Int. Ed. Engl.* **2011**, *50*, 260.
51. Young-Hoon, Y.; Kab-Young, K.; Un-Kyu, P. *Ceram. Int.* **2012**, *38*, 1599.
52. Mills, A.; Williams, F. C. *Thin Solid Films* **1996**, *306*, 163.
53. Yoshinaga, T.; Tanaka, Y.; Ichimura, T.; Hiratsuka, H.; Kobayashi, M.; Hoshi, T. *J. Lumin.* **1998**, *78*, 221.
54. Hu, S.-R.; Liu, J.-M.; Yang, T.-L.; Liu, H.-Z.; Huang, J.-L.; Lin, Q.-W.; Zhu, G.-H.; Huang, X.-M. *Microchim. Acta* **2005**, *152*, 53.
55. Bomm, J.; Büchtemann, A.; Fiore, A.; Manna, L.; Nelson, J. H.; Hill, D.; van Sark, W. G. J. H. M. *Beilstein J. Nanotechnol.* **2010**, *1*, 94.
56. Liu, J.-M.; Huang, X.-M.; Zhang, L.-H.; Zheng, Z.-Y.; Lin, X.; Zhang, X.-Y.; Jiao, L.; Cui, M.-L.; Jiang, S.-L.; Lin, S.-Q. *Anal. Chim. Acta* **2012**, *744*, 60.
57. Liu, J.-M.; Wu, A.-H.; Xu, H.-H.; Wang, Q.-H.; Li, L.-D.; Zhu, G.-H. *Talanta* **2005**, *65*, 501.
58. Jiaming, L.; Wenqi, L.; Xuelin, L.; Hailing, C.; Qiaomei, L.; Longdi, L.; Zhimin, L.; Guohui, Z.; Cuilian, C. *Spectrochim. Acta Part A* **2005**, *61*, 3077.
59. Nadagouda, M. N.; Varma, R. S. *Biomacromolecules* **2007**, *8*, 2762.
60. Luna-Martínez, J. F.; Hernández-Uresti, D. B.; Reyes-Melo, M. E.; Guerrero-Salazar, C. A.; González-González, V. A.; Sepúlveda-Guzmán, S. *Carbohydr. Polym.* **2011**, *84*, 566.
61. Tang, C.-R.; Su, Z.; Lin, B.-G.; Huang, H.-W.; Zeng, Y.-L.; Li, S.; Huang, H.; Wang, Y.-J.; Li, C.-X.; Shen, G.-L.; Yu, R.-Q. *Anal. Chim. Acta* **2010**, *678*, 203.
62. Deligne, N.; Lamme, J.; Devillers, M. *Eur. J. Inorg. Chem.* **2011**, 2011, 3461.
63. Wang, H.; Shao, Z.; Chen, B.; Zhang, T.; Wang, F.; Zhong, H. *RSC Adv.* **2012**, *2*, 2675.
64. Zhao, C.; Egashira, N.; Kurauchi, Y.; Ohga, K. *Electrochim. Acta* **1998**, *43*, 2167.
65. Qu, Y.; Liu, X.; Zheng, X.; Guo, Z. *Anal. Sci.* **2012**, *28*, 571.
66. Cai, Z.; Wu, Y.; Huang, Y.; Li, Q.; Chen, X.; Chen, X. *Talanta* **2012**, *94*, 356.
67. Zhang, M.; Dai, W.; Yan, M.; Ge, S.; Yu, J.; Song, X.; Xu, W. *Analyst* **2012**, *137*, 2112.
68. Zhao, J.; Chen, M.; Yu, C.; Tu, Y. *Analyst* **2011**, *136*, 4070.
69. Jie, G.; Zhang, J.; Wang, D.; Cheng, C.; Chen, H.; Zhu, J. *Anal. Chem.* **2008**, *80*, 4033.
70. Wang, T.; Zhang, S.; Mao, C.; Song, J.; Niu, H.; Jin, B.; Tian, Y. *Biosens. Bioelectron.* **2012**, *31*, 369.
71. Wu, Y.; Xue, P.; Kang, Y.; Hui, K. M. *Anal. Chem.* **2013**, *85*, 3166.
72. Tsvirko, M.; Mandowska, E.; Biernacka, M.; Tkaczyk, S.; Mandowski, A. *J. Lumin.* **2013**, *143*, 128.

73. Kumar, H.; Srivastava, R.; Dutta, P. K. *Carbohydr. Polym.* **2013**, *97*, 327.
74. George, A.; Shibu, E. S.; Maliyekkal, S. M.; Bootharaju, M. S.; Pradeep, T. *ACS Appl. Mater. Interfaces* **2012**, *4*, 639.
75. Sreeprasad, T. S.; Maliyekkal, M. S.; Deepti, K.; Chaudhari, K.; Xavier, P. L.; Pradeep, T. *ACS Appl. Mater. Interfaces* **2011**, *3*, 2643.
76. Nie, Q.; Tan, W. B.; Zhang, Y. *Nanotechnology* **2006**, *17*, 140.
77. Tan, W. B.; Huang, N.; Zhang, Y. *J. Colloid Interface Sci.* **2007**, *310*, 464.
78. Zhao, Q.; Rong, X.; Chen, L.; Ma, H.; Tao, G. *Talanta* **2013**, *114*, 110.
79. Chelebaeva, E.; Larionova, J.; Guari, Y.; Ferreira, R. A. S.; Carlos, L. D.; Trifonov, A. A.; Kalaivani, T.; Lascialfari, A.; Guérin, C.; Molvinger, K.; Datas, L.; Maynadier, M.; Gary-Bobo, M.; Garcia, M. *Nanoscale* **2011**, *3*, 1200.
80. Wang, F.; Zhang, Y.; Fan, X.; Wang, M. *Nanotechnology* **2006**, *17*, 1527.
81. Chen, Q.; Wang, X.; Chen, F.; Zhang, Q.; Dong, B.; Yang, H.; Liu, G.; Zhu, Y. *J. Mater. Chem.* **2011**, *21*, 7661.
82. Liu, F.; Carlos, L. D.; Ferreira, R. A. S.; Rocha, J.; Ferro, M. C.; Tourrette, A.; Quignard, F.; Robitzer, M. *J. Phys. Chem. B* **2010**, *114*, 77.
83. Yan, C.; Jiao, L.; Guo, C.; Zhang, M.; Qiu, G. *J. Rare Earths* **2008**, *26*, 660.
84. Wang, C.; Huang, Y. *New J. Chem.* **2014**, *38*, 657.
85. Shen, J.-M.; Xu, L.; Lu, Y.; Cao, H.-M.; Xu, Z.-G.; Chen, T.; Zhang, H.-X. *Int. J. Pharm.* **2012**, *427*, 400.
86. Shen, J.-M.; Guan, X.-M.; Liu, X.-Y.; Lan, J.-F.; Cheng, T.; Zhang, H.-X. *Bioconjugate Chem.* **2012**, *23*, 1010.
87. Guo, J.; Wang, C.; Mao, W.; Yang, W.; Liu, C.; Chen, J. *Nanotechnology* **2008**, *19*, 315605.
88. Sandros, M. G.; Behrendt, M.; Maysinger, D.; Tabrizian, M. *Adv. Funct. Mater.* **2007**, *17*, 3724.
89. Deng, D.; Qu, L.; Zhang, J.; Ma, Y.; Gu, Y. *ACS Appl. Mater. Interfaces* **2013**, *5*, 10858.
90. Ramanery, F. P.; Mansur, A. A.; Mansur, H. S. *Nanoscale Res. Lett.* **2013**, *8*, 512.
91. Mazumder, S.; Sarkar, J.; Dey, R.; Mitra, M. K.; Mukherjee, S.; Das, G. C. *J. Exp. Nanosci.* **2010**, *5*, 438.
92. Saeed, S. E.-S.; El-Molla, M. M.; Hassan, M. L.; Bakir, E.; Abdel-Mottaleb, M. M. S.; Abdel-Mottaleb, M. S. A. *Carbohydr. Polym.* **2014**, *99*, 817.
93. Vasimalai, N.; Abraham John, S. *Talanta* **2013**, *115*, 24.
94. Huang, N. M.; Radiman, S.; Lim, H. N.; Yeong, S. K.; Khiew, P. S.; Chiu, W. S.; Saeed, G. H. M.; Nadarajah, K. *Chem. Eng. J.* **2009**, *147*, 399.
95. Charan, S.; Sanjiv, K.; Singh, N.; Chien, F.-C.; Chen, Y.-F.; Nergui, N. N.; Huang, S.-H.; Kuo, C. W.; Lee, T.-C.; Chen, P. *Bioconjugate Chem.* **2012**, *23*, 2173.
96. Abdelhamid, H. N.; Wu, H.-F. *J. Mater. Chem. B* **2013**, *1*, 6094.
97. Li, H.; Wang, L. *Chin. Sci. Bull.* **2013**, *58*, 4051.
98. He, Z.; Zhu, H.; Zhou, P. *J. Fluoresc.* **2012**, *22*, 193.
99. Xie, M.; Liu, H.-H.; Chen, P.; Zhang, Z.-L.; Wang, X.-H.; Xie, Z.-X.; Du, Y.-M.; Pan, B.-Q.; Pang, D.-W. *Chem. Commun.* **2005**, 5518.
100. Wang, X. *J. Nanosci. Nanotechnol.* **2009**, *9*, 6866.
101. Pinto, R. J. B.; Granadeiro, C. M.; Freire, C. S. R.; Silvestre, A. J. D.; Neto, C. P.; Ferreira, R. A. S.; Carlos, L. D.; Cavaleiro, A. M. V.; Trindade, T.; Nogueira, H. I. S. *Eur. J. Inorg. Chem.* **2013**, 2013, 1890.
102. Gleitsmann, T.; Bernhardt, T. M.; Wöste, L. *Appl. Phys. A* **2005**, *82*, 125.
103. Kim, Y.; Minami, N.; Kazaoui, S. *Appl. Phys. Lett.* **2005**, *86*, 073103.
104. Borkovska, L. V.; Korsunska, N. O.; Stara, T. R.; Dzhagan, V. M.; Stroyuk, O. L.; Raevska, O. Y.; Kryshtab, T. G. *Phys. Status Solidi* **2012**, *9*, 1779.
105. Raevskaya, A. E.; Stroyuk, A. L.; Kuchmiy, S. Y.; Dzhagan, V. M.; Valakh, M. Y.; Zahn, D. R. T. *J. Phys. Condens. Matter* **2007**, *19*, 386237.
106. Efendiev, T. S.; Kruchenok, J. V.; Rubinov, A. N. *J. Appl. Spectrosc.* **2013**, *80*, 142.
107. Hou, Z.; Li, X.; Li, C.; Dai, Y.; Ma, P.; Zhang, X.; Kang, X.; Cheng, Z.; Lin, J. *Langmuir* **2013**, *29*, 9473.
108. Wang, Y.; Chen, H.; Ye, C.; Hu, Y. *Mater. Lett.* **2008**, *62*, 3382.
109. Girija Aswathy, R.; Sivakumar, B.; Brahatheeshwaran, D.; Ukai, T.; Yoshida, Y.; Maekawa, T.; Kumar, S. D. *Mater. Express* **2011**, *1*, 291.
110. Gerard, V. A.; Gun'ko, Y. K.; Prasad, B. R.; Rochev, Y. *Methods Mol. Biol.* **2012**, *906*, 275.
111. Li, C.; Wang, X.; Ye, C.; Wang, Y.; Hu, Y.; Yan, Z. *J. Nanosci. Nanotechnol.* **2013**, *13*, 4330.
112. Skobeeva, V. M.; Smyntyna, V. A.; Sviridova, O. I.; Struts, D. A.; Tyurin, A. V. *J. Appl. Spectrosc.* **2008**, *75*, 576.
113. Azhniuk, Y. M.; Dzhagan, V. M.; Raevskaya, A. E.; Stroyuk, A. L.; Kuchmiy, S. Y.; Valakh, M. Y.; Zahn, D. R. T. *J. Phys. Condens. Matter* **2008**, *20*, 455203.
114. Sapozhnikova, V.; Willsey, B.; Asmis, R.; Wang, T.; Jenkins, J. T.; Mancuso, J.; Ma, L. L.; Kuranov, R.; Milner, T. E.; Johnston, K.; Feldman, M. D. *J. Biomed. Opt.* **2012**, *17*, 026006.
115. Zhong, S.-L.; Zhang, L.-F.; Jiang, J.-W.; Lv, Y.-H.; Xu, R.; Xu, A.-W.; Wang, S.-P. *CrystEngComm* **2011**, *13*, 4151.
116. Liang, Q.; Ma, W.; Shi, Y.; Li, Z.; Yang, X. *Carbon* **2013**, *60*, 421.
117. Guan, X.; Su, Z. *Polym. Adv. Technol.* **2008**, *19*, 385.
118. Zhang, J.; Li, Q.; Di, X.; Liu, Z.; Xu, G. *Nanotechnology* **2008**, *19*, 435606.
119. Zhang, H.; Fu, X.; Niu, S.; Xin, Q. *J. Alloys Compd.* **2008**, *457*, 61.
120. Mishra, P.; Yadav, R. S.; Pandey, A. C. *Ultrason. Sonochem.* **2010**, *17*, 560.

121. Zamiri, R.; Zakaria, A.; Ahangar, H. A.; Darroudi, M.; Zak, A. K.; Drummen, G. P. C. *J. Alloys Compd.* **2012**, *516*, 41.

122. Oluwafemi, O. S. *Colloids Surf. B* **2009**, *73*, 382.

123. Li, J.; Xu, J.; Zhao, L.; Xu, Q.; Fang, G. *Mater. Res. Bull.* **2013**, *48*, 1560.

124. Leones, R.; Rodrigues, L. C.; Fernandes, M.; Ferreira, R. A. S.; Cesarino, I.; Pawlicka, A.; Carlos, L. D.; Bermudez, V. Z.; Silva, M. M. *J. Electroanal. Chem.* **2013**, *708*, 116.

125. Liu, F.; Carlos, L. D.; Ferreira, R. A. S.; Rocha, J.; Gaudino, M. C.; Robitzer, M.; Quignard, F. *Biomacromolecules* **2008**, *9*, 1945.

126. Bardajee, G. R.; Hooshyar, Z.; Rostami, I. *Colloids Surf. B* **2011**, *88*, 202.

127. Liu, J.; Zhang, Y.; Yan, C.; Wang, C.; Xu, R.; Gu, N. *Langmuir* **2010**, *26*, 19066.

128. Ramos, A. P.; Gonçalves, R. R.; Serra, O. A.; Zaniquelli, M. E. D.; Wong, K. *J. Lumin.* **2007**, *127*, 461.

129. Luz, P. P.; Pires, A. M.; Serra, O. A. *J. Fluoresc.* **2008**, *18*, 695.

130. Kumar, M. N. V. R.; Muzzarelli, R. A. A.; Muzzarelli, C.; Sashiwa, H.; Domb, A. *J. Chem. Rev.* **2004**, *104*, 6017.